

<sup>1</sup> **Title:** Carbon cycling in mature and regrowth forests globally: a macroecological synthesis based on the  
<sup>2</sup> global Forest Carbon (ForC) database

<sup>3</sup> **Authors:**

<sup>4</sup> Kristina J. Anderson-Teixeira<sup>1,2\*</sup>

<sup>5</sup> Valentine Herrmann<sup>1</sup>

<sup>6</sup> Becky Banbury Morgan<sup>3</sup>

<sup>7</sup> Ben Bond-Lamberty<sup>4</sup>

<sup>8</sup> Susan C. Cook-Patton<sup>5</sup>

<sup>9</sup> Abigail E. Ferson<sup>1,6</sup>

<sup>10</sup> Helene C. Muller-Landau<sup>1</sup>

<sup>11</sup> Maria M. H. Wang<sup>1,7</sup>

<sup>12</sup> **Author Affiliations:**

<sup>13</sup> 1. Conservation Ecology Center; Smithsonian Conservation Biology Institute; National Zoological Park,  
<sup>14</sup> Front Royal, VA 22630, USA

<sup>15</sup> 2. Center for Tropical Forest Science-Forest Global Earth Observatory; Smithsonian Tropical Research  
<sup>16</sup> Institute; Panama, Republic of Panama

<sup>17</sup> 3. School of Geography, University of Leeds, Leeds, UK

<sup>18</sup> 4. Joint Global Change Research Institute, Pacific Northwest National Laboratory, College Park  
<sup>19</sup> Maryland 20740, USA

<sup>20</sup> 5. The Nature Conservancy; Arlington VA 22203, USA

<sup>21</sup> 6. College of Natural Resources, University of Idaho; Moscow, Idaho 83843, USA

<sup>22</sup> 7. Grantham Centre for Sustainable Futures and Department of Animal and Plant Sciences, University of  
<sup>23</sup> Sheffield, Western Bank, Sheffield, South Yorkshire S10 2TN, UK

<sup>24</sup> \*corresponding author: teixeirak@si.edu; +1 540 635 6546

<sup>25</sup> **NOTES TO COAUTHORS:**

- <sup>26</sup> • “???” indicates a reference that we have entered in the .Rmd file, but not yet in the bibliography file.  
<sup>27</sup> Don’t worry about those. (However, places with “REF” need references)
- <sup>28</sup> • bold/ italic text indicates places where I know we need to go back and revisit/ fill in info

**29    Summary**

**30    Background.** Earth's climate is closely linked to forests, which strongly influence atmospheric carbon dioxide  
**31** ( $\text{CO}_2$ ) and climate by their impact on the global carbon (C) cycle. However, efforts to incorporate forests  
**32** into climate models and  $\text{CO}_2$  accounting frameworks have been constrained by a lack of accessible,  
**33** global-scale data on how C cycling varies across forest types and stand ages.

**34    Methods/Design.** Here, we draw from the Global Forest Carbon Database, ForC, to provide a macroscopic  
**35** overview of C cycling in the world's forests, giving special attention to stand age-related variation.

**36** Specifically, we use 11923 *ForC* records from 865 geographic locations representing 34 C cycle variables to  
**37** characterize ensemble C budgets for four broad forest types (tropical broadleaf evergreen, temperate  
**38** broadleaf, temperate conifer, and taiga), including estimates for both mature and regrowth (age <100 years)  
**39** forests. For regrowth forests, we quantify age trends for all variables.

**40    Review Results/ Synthesis.** *ForC v3.0* yielded a fairly comprehensive picture of C cycling in the world's  
**41** major forest biomes, with broad closure of C budgets. The rate of C cycling generally increased from boreal  
**42** to tropical regions in both mature and regrowth forests, whereas C stocks showed less directional variation.  
**43** The majority of flux variables, together with most live biomass pools, increased significantly with stand age,  
**44** and the rate of increase again tended to increase from boreal to tropical regions.

**45    Discussion. NEED TO WRITE THIS!!!**

**46    Key words:** forest ecosystems; carbon cycle; stand age; productivity; respiration; biomass; global

47 **Background**

48 Forest ecosystems are shaping the course of climate change (IPCC1.5) through their influence on atmospheric  
49 carbon dioxide (CO<sub>2</sub>). Despite the centrality of forest C cycling in regulating atmospheric CO<sub>2</sub>, important  
50 uncertainties in climate models (???, ???, ???, Krause *et al* 2018) and CO<sub>2</sub> accounting frameworks (Pan *et*  
51 *al* 2011) can be traced to lack of accessible, comprehensive data on how C cycling varies across forest types  
52 and in relation to stand history. These require large-scale databases with global coverage, which runs  
53 contrary to the nature in which forest C stocks and fluxes are measured and published. While remote sensing  
54 measurements are increasingly useful for global- or regional-scale estimates of a few critical variables [e.g.,  
55 aboveground biomass: (???); **REF**; gross primary productivity, *GPP*: Li and Xiao (2019); **REFS for**  
56 **biomass change, net CO2 flux**], measurement of most forest C stocks and fluxes require intensive  
57 on-the-ground data collection. Here, we provide a robust and comprehensive analysis of carbon cycling from  
58 a stand to global level, and by biome and stand age, using the largest global compilation of forest carbon  
59 data, which is available in our open source Global Carbon Forest database (ForC; Fig. 1).

60 A robust understanding of forest impacts on global C cycling is essential. Annual gross CO<sub>2</sub> sequestration in  
61 forests (gross primary productivity, *GPP*) is estimated at >69 Gt C yr<sup>-1</sup> (???), or >7 times average annual  
62 fossil fuel emissions from 2009-2018 ( $9.5 \pm 0.5$  Gt C yr<sup>-1</sup>; ???). Most of this enormous C sequestration is  
63 counterbalanced by CO<sub>2</sub> releases to the atmosphere through ecosystem respiration (*R<sub>eco</sub>*) or fire, with forests  
64 globally dominant as sources of both soil respiration (???) and fire emissions (REF). (check if  
65 **deforestation statistic below includes natural fire, exclude here if it does.**) In recent years, the  
66 remaining CO<sub>2</sub> sink averaged  $3.2 \pm 0.6$  GtC yr<sup>-1</sup> from 2009-2018, offsetting 29% of anthropogenic fossil fuel  
67 emissions (???). Yet, this sink is reduced by *deforestation/ forest losses to anthropogenic and natural*  
68 *disturbances*. Recent net deforestation (*i.e.*, gross deforestation minus regrowth) has been a source of CO<sub>2</sub>  
69 emissions, estimated at ~1.1 Gt C yr<sup>-1</sup> from YEAR-YEAR (Pan *et al* 2011; **UPDATE**), reducing the net  
70 forest sink to ~1.1-2.2 Gt C yr<sup>-1</sup> across Earth's forests (???).

71 The future of the current forest C sink is dependent both upon forest responses to climate change itself and  
72 human land use decisions, which will feedback and strongly influence the course of climate change.  
73 Regrowing forests in particular will play an important role (Pugh *et al* 2019), as these represent a large  
74 (~#%) and growing proportion of Earth's forests (McDowell *et al* 2020). Understanding, modeling, and  
75 managing forest-atmosphere CO<sub>2</sub> exchange is thus central to efforts to mitigate climate change [Grassi *et al*  
76 (2017); Griscom *et al* (2017); **Cavaleri et al 2015**].

77 Despite the importance of forests, comprehensive global studies have historically been limited by the scattered  
78 and more local nature of research studies. Primary research articles typically cover only a small numbers of  
79 sites at a time. The rare exceptions that span regions or continents with rare exceptions spanning regions or  
80 continents are typically coordinated through research networks such as ForestGEO (Anderson-Teixeira *et al*  
81 2015, e.g., Lutz *et al* 2018) or FLUXNET [Baldocchi *et al* (2001); e.g., **FLUXNET\_REF**]. The result of  
82 decades of research on forest C cycling is that tens of thousands of records have been distributed across  
83 literally thousands of scientific articles –often behind paywalls– along with variation in data formats, units,  
84 measurement methods, *etc..* In this format, the data are effectively inaccessible for many global-scale  
85 analyses, including those attempting to benchmark model performance with global data (Clark *et al* 2017,  
86 Luo *et al* 2012), quantify the the role of forests in the global C cycle (*e.g.*, Pan *et al* 2011), or use  
87 book-keeping methods to quantify actual or scenario-based exchanges of CO<sub>2</sub> between forests and the  
88 atmosphere [Griscom *et al* (2017); **REFS**]. Scattered data are not conducive for advancing science nor for

89 making decisions about how to best manage our forests as a tool for constraining the climate crisis.

90 To address the need for global-scale analyses of forest C cycling, we recently developed *ForC*

91 (Anderson-Teixeira *et al* 2016, pp @anderson-teixeira\_forc\_2018). *ForC* contains published estimates of

92 forest ecosystem C stocks and annual fluxes (>50 variables), with the different variables capturing the unique

93 ecosystem pools (e.g., woody, foliage, and root biomass; dead wood) and flux types (e.g, gross and net

94 primary productivity; soil, root, and ecosystem respiration). These data are ground-based measurements,

95 and *ForC* contains associated data required for interpretation (e.g., stand history, measurement methods).

96 These data have been amalgamated from original peer-reviewed publications, either directly or via

97 intermediary data compilations. Since its most recent publication (Anderson-Teixeira *et al* 2018), *ForC*

98 has grown to include two additional large databases: the Global Soil Respiration Database (SRDB;

99 Bond-Lamberty and Thomson 2010) and the Global Reforestation Opportunity Assessment database

100 (GROA; Cook-Patton *et al* 2020) that also synthesized published forest C data. Following these additions,

101 *ForC* currently contains 39762 records from 10608 plots and 1532 distinct geographic areas representing all

102 forested biogeographic and climate zones. This represents an 129% increase in records from the prior

103 publication (Anderson-Teixeira *et al* 2018).

104 Here, we analyze the more extensive *ForC* data (Fig. 1) to provide a robust overview of stand-level carbon

105 cycling of the world's major forest biomes and how it varies with stand age. Our primary goal is to provide a

106 data-driven summary of our current state of knowledge on broad trends in forest C cycling. Specifically, we

107 address three broad questions:

108 1. How thoroughly can we represent C budgets for each of the world's major forest biomes (*i.e.*, tropical,

109 temperate broadleaf and deciduous, boreal) based on the current *ForC* data?

110 2. How do C cycling vary across the world's major forest biomes?

111 3. How does C cycling vary with stand age (in interaction with biome)?

112 While components of these questions have been previously addressed (Luyssaert *et al* 2007,

113 Anderson-Teixeira *et al* 2016, Cook-Patton *et al* 2020, Banbury Morgan *et al* n.d.), our analysis represents

114 by far the most comprehensive analysis of C cycling in global forests, and will serve as a foundation for

115 improved understanding of global forest C cycling and highlight where key sources of uncertainty still reside.

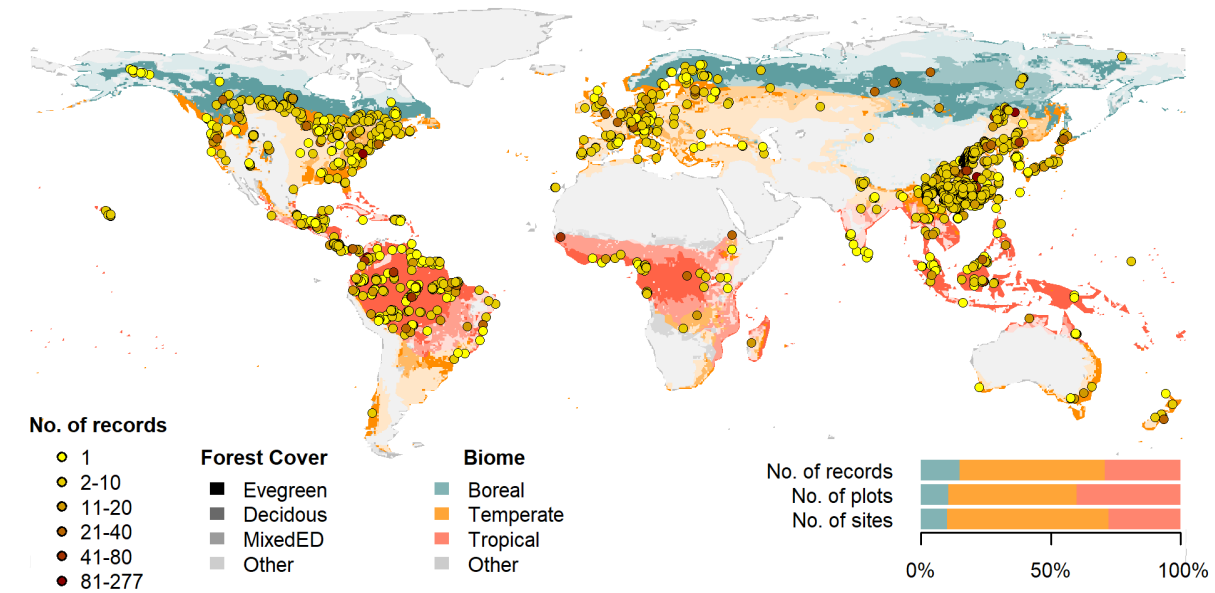


Figure 1 | Map of sites included in this analysis. Symbols are colored according to the number of records at each site. Underlying map shows coverage of evergreen, deciduous, and mixed forests (from SYNMAP; Jung et al. 2006) and biomes. Distribution of sites, plots, and records among biomes is shown in the inset.

## 116 Methods/ Design

117 This review synthesizes data from the *ForC* database (Fig. 1; <https://github.com/forc-db/ForC>;  
 118 Anderson-Teixeira *et al* 2016, pp @anderson-teixeira\_forc\_2018). *ForC* amalgamates numerous  
 119 intermediary data sets (*e.g.*, Luyssaert *et al* 2007, Bond-Lamberty and Thomson 2010, Cook-Patton *et al*  
 120 2020) and original studies. Original publications were referenced to check values and obtain information not  
 121 contained in intermediary data sets, although this process has not been completed for all records. The  
 122 database was developed with goals of understanding how C cycling in forests varies across broad geographic  
 123 scales and as a function of stand age. As such, there has been a focus on incorporating data from regrowth  
 124 forests (*e.g.*, Anderson *et al* 2006, Martin *et al* 2013, Bonner *et al* 2013) and obtaining stand age data when  
 125 possible (83% of records in v.2.0; Anderson-Teixeira *et al* 2018). Particular attention was given to developing  
 126 the database for tropical forests (Anderson-Teixeira *et al* 2016), which represented roughly one-third of  
 127 records in *ForC* v.2.0\* (Anderson-Teixeira *et al* 2018). Since publication of *ForC* v.2.0, we added the  
 128 following data to *ForC*: the Global Database of Soil Respiration Database (*SRDB* v.##, 9488 records;  
 129 Bond-Lamberty and Thomson 2010), the Global Reforestation Opportunity Assessment database (*GROA*  
 130 v1.0, 10116 records; Cook-Patton *et al* 2020, Anderson-Teixeira *et al* 2020). We've also added data from  
 131 individual publications (detailed list at [https://github.com/forc-  
 132 db/ForC/blob/master/database\\_management\\_records/ForC\\_data\\_additions\\_log.csv](https://github.com/forc-db/ForC/blob/master/database_management_records/ForC_data_additions_log.csv)), with a particular  
 133 focus on productivity (Banbury Morgan *et al* n.d., *e.g.*, Taylor *et al* 2017), dead wood, and ForestGEO sites  
 134 (*e.g.*, Lutz *et al* 2018, p @johnson\_climate\_2018). We note that there remains a significant amount of  
 135 relevant data that is not yet included in *ForC*, particularly biomass data from national forest inventories

136 (e.g.,; **REFS**). The database version used for this analysis has been tagged as a new release on Github (**XX**)  
137 and assigned a DOI through Zenodo (DOI: TBD).

138 To facilitate analyses, we created a simplified version of ForC, *ForC-simplified*  
139 ([https://github.com/forc-db/ForC/blob/master/ForC\\_simplified](https://github.com/forc-db/ForC/blob/master/ForC_simplified)), which we analyzed here. In generating  
140 *ForC-simplified*, all measurements originally expressed in units of dry organic matter (*OM*) were converted  
141 to units of C using the IPCC default of  $C = 0.47 * OM$  (IPCC 2006). Duplicate or otherwise conflicting  
142 records were reconciled as described in APPENDIX S1, resulting in a total of 32499 records (81.7% size of  
143 total database). Records were filtered to remove plots that had undergone significant anthropogenic  
144 management or major disturbance since the most recent stand initiation event. Specifically, we removed all  
145 plots flagged as managed in ForC-simplified (18.9%). This included plots with any record of managements  
146 manipulating CO<sub>2</sub>, temperature, hydrology, nutrients, or biota, as well as any plots whose site or plot name  
147 contained the terms “plantation”, “planted”, “managed”, “irrigated”, or “fertilized”. Plots flagged as  
148 disturbed in ForC-simplified (5.7%) included stands that had undergone any notable anthropogenic thinning  
149 or partial harvest. We retained sites that were grazed or had undergone low severity natural disturbances  
150 (<10% mortality) including droughts, major storms, fires, and floods. We removed all plots for which no  
151 stand history information had been retrieved (7.3%). In total, this resulted in 23199 records (58.3% of the  
152 records in the database) being eligible for inclusion in the analysis.

153 We selected 23 annual flux and 11 C stock variables for inclusion in the analysis. These different flux and  
154 stock variables (Table 1) represent different pools (e.g., aboveground biomass, dead wood, ecosystem total)  
155 and levels of combination (e.g., total aboveground net primary productivity (*ANPP*) versus the ANPP of  
156 individual elements such as foliage, roots, and branches. Note that two flux variables, aboveground  
157 heterotrophic ( $R_{het-ag}$ ) and total ( $R_{het}$ ) respiration, were included for conceptual completeness but had no  
158 records in *ForC* (Table 1). Records for these variables represented 67.5% of the total records eligible for  
159 inclusion. For this analysis, we combined some of ForC’s specific variables (e.g., multiple variables for net  
160 primary productivity, such as measurements including or excluding fruit and flower production and herbivory)  
161 into more broadly defined variables. Specifically, net ecosystem exchange (measured by eddy-covariance;  
162 **FLUXNET REF**) and biometric estimates of *NEP* were combined into the single variable *NEP* (Table 1).  
163 Furthermore, for *NPP*, *ANPP*, and *ANPP<sub>litterfall</sub>*, *ForC* variables specifying inclusion of different  
164 components were combined. Throughout ForC, for all measurements drawing from tree census data (e.g.,  
165 biomass, productivity), the minimum diameter breast height (DBH) threshold for tree census was  $\leq 10\text{cm}$ .  
166 All records were measured directly or derived from field measurements (as opposed to modeled).

167 For this analysis, we grouped forests into four broad biome types based on climate zones and dominant  
168 vegetation type (tropical broadleaf, temperate broadleaf, temperate needleleaf, and boreal needleleaf) and  
169 two age classifications (young and mature). Climate zones (Fig. 1) were defined based on site geographic  
170 coordinates according to Köppen-Geiger zones (Rubel and Kottek 2010). We defined the tropical biome as  
171 including all equatorial (A) zones, temperate biomes as including all warm temperate (C) zones and warmer  
172 snow climates (Dsa, Dsb, Dwa, Dwb, Dfa, and Dfb), and the boreal biome as including the colder snow  
173 climates (Dsc, Dsd, Dwc, Dwd, Dfc, and Dfd). Any forests in dry (B) and polar (E) Köppen-Geiger zones  
174 were excluded from the analysis. We defined leaf type (broadleaf / needleleaf) was based on descriptions in  
175 original publications (prioritized) or values extracted from a global map based on satellite observations  
176 (SYNMAP; ???). For young tropical forests imported from *GROA* but not yet classified by leaf type, we  
177 assumed that all were broadleaf, consistent with the rarity of naturally regenerating needleleaf forests in the

Table 1. Carbon cycle variables included in this analysis, their sample sizes, and summary of biome differences and age trends.

Variable	Description	N records			biome differences*	age trend†
		records	plots	geographic areas		
<b>Annual fluxes</b>						
<i>NEP</i>	net ecosystem production or net ecosystem exchange (+ indicates C sink)	329	146	88	n.s.	+; xB
<i>GPP</i>	gross primary production ( $NPP + R_{auto}$ or $R_{eco} - NEE$ )	303	115	84	TrB > TeB $\geq$ TeN $\geq$ BoN	+; xB
<i>NPP</i>	net primary production ( $ANPP + BNPP$ )	214	112	74	TrB > TeB $\geq$ TeN $>$ BoN	n.s.
<i>ANPP</i>	aboveground <i>NPP</i>	343	236	131	TrB > TeB $\geq$ TeN $>$ BoN	+; xB
<i>ANPP<sub>woody</sub></i>	woody production ( $ANPP_{stem} + ANPP_{branch}$ )	64	53	37	n.s.	+
<i>ANPP<sub>stem</sub></i>	woody stem production	217	190	117	TrB > TeN $\geq$ TeB $\geq$ BoN	n.s.
<i>ANPP<sub>branch</sub></i>	branch turnover	69	59	42	TrB > TeB $\geq$ TeN	n.s.
<i>ANPP<sub>foliage</sub></i>	foliage production, typically estimated as annual leaf litterfall	162	132	88	TrB > TeB $\geq$ TeN $>$ BoN	+
<i>ANPP<sub>litterfall</sub></i>	litterfall, including leaves, reproductive structures, twigs, and sometimes branches	82	70	55	n.s.	+
<i>ANPP<sub>repro</sub></i>	production of reproductive structures (flowers, fruits, seeds)	51	44	34	n.t.	n.t.
<i>ANPP<sub>folivory</sub></i>	foliar biomass consumed by folivores	20	12	11	n.t.	n.t.
<i>M<sub>woody</sub></i>	woody mortality—i.e., $B_{ag}$ of trees that die	18	18	18	n.t.	n.t.
<i>BNPP</i>	belowground NPP ( $BNPP_{coarse} + BNPP_{fine}$ )	148	116	79	TrB > TeN $\geq$ TeB $\geq$ BoN	+
<i>BNPP<sub>coarse</sub></i>	coarse root production	77	56	36	TeN $\geq$ TrB	n.s.
<i>BNPP<sub>fine</sub></i>	fine root production	123	99	66	n.s.	+
<i>R<sub>eco</sub></i>	ecosystem respiration ( $R_{auto} + R_{het}$ )	213	98	70	TrB > TeB $\geq$ TeN	+
<i>R<sub>auto</sub></i>	autotrophic respiration ( $(R_{auto-ag} + R_{root})$ )	24	23	15	n.t.	n.t.
<i>R<sub>auto-ag</sub></i>	aboveground autotrophic respiration (i.e., leaves and stems)	2	2	1	n.t.	n.t.
<i>R<sub>root</sub></i>	root respiration	181	139	95	TrB $\geq$ TeB	+
<i>R<sub>soil</sub></i>	soil respiration ( $(R_{het-soil} + R_{root})$ )	627	411	229	TrB > TeB $>$ TeN $\geq$ BoN	n.s.
<i>R<sub>het-soil</sub></i>	soil heterotrophic respiration	197	156	100	TrB > TeB $\geq$ TeN	n.s.
<i>R<sub>het-ag</sub></i>	aboveground heterotrophic respiration	0	0	0	-	-
<i>R<sub>het</sub></i>	heterotrophic respiration ( $(R_{het-ag} + R_{het-soil})$ )	0	0	0	-	-
<b>Stocks</b>						
<i>B<sub>tot</sub></i>	total live biomass ( $B_{ag} + B_{root}$ )	188	157	87	TrB $\geq$ TeB $>$ BoN	+; xB
<i>B<sub>ag</sub></i>	aboveground live biomass ( $B_{ag-wood} + B_{foliage}$ )	4466	4072	621	TrB $\geq$ TeN $\geq$ TeB $>$ BoN	+; xB
<i>B<sub>ag-wood</sub></i>	woody component of aboveground biomass	115	102	64	TeN $>$ TrB $\geq$ BoN	+; xB
<i>B<sub>foliage</sub></i>	foliage biomass	134	115	72	TeN $>$ TrB $\geq$ BoN $\geq$ TeB	+; xB
<i>B<sub>root</sub></i>	total root biomass ( $(B_{root-coarse} + B_{root-fine})$ )	2329	2298	360	n.s.	+; xB
<i>B<sub>root-coarse</sub></i>	coarse root biomass	134	120	73	TeN $>$ TeB $\geq$ BoN	+; xB
<i>B<sub>root-fine</sub></i>	fine root biomass	226	180	109	n.s.	+; xB
<i>DW<sub>tot</sub></i>	deadwood ( $DW_{standing} + DW_{down}$ )	79	73	42	n.t.	+; xB
<i>DW<sub>standing</sub></i>	standing dead wood	36	35	22	n.t.	n.t.
<i>DW<sub>down</sub></i>	fallen dead wood, including coarse and sometimes fine woody debris	278	265	37	n.t.	+; xB
<i>OL</i>	organic layer / litter/ forest floor	474	413	115	n.s.	+; xB

\* Tr: Tropical, TeB: Temperate Broadleaf, TeN: Temperate Needleleaf, B: Boreal, n.s.: no significant differences, n.t.: not tested

† + or -: significant positive or negative trend, xB: significant age x biome interaction, n.s.: no significant age trend, n.t.: not tested

tropics (REF). We also classified forests as “young” (< 100 years) or “mature” ( $\geq 100$  years or classified as “mature”, “old growth”, “intact”, or “undisturbed” in original publication). Assigning stands to these

180 groupings required the exclusion of records for which *ForC* lacked geographic coordinates (0.4% of sites in  
181 full database) or records of stand age (5.7% of records in full database). We also excluded records of stand  
182 age = 0 year (0.8% of records in full database). In total, our analysis retained 76.1 of the focal variable  
183 records for forests of known age. Numbers of records by biome and age class are given in Table S1.

184 Data were summarized to produce schematics of C cycling across the eight biome by age group combinations  
185 identified above. To obtain the values reported in the C cycle schematics, we first averaged any repeated  
186 measurements within a plot. Values were then averaged across geographically distinct areas, defined as plots  
187 clustered within 25 km of one another (*sensu* Anderson-Teixeira *et al* 2018), weighting by area sampled if  
188 available for all records. This step was taken to avoid pseudo-replication and to combine any records from  
189 sites with more than one name in ForC.

190 We tested whether the C budgets described above “closed”—*i.e.*, whether they were internally consistent.  
191 Specifically, we first defined relationships among variables: for example,  $NEP = GPP - R_{eco}$ ,  
192  $BNPP = BNPP_{coarse} + BNPP_{fine}$ ,  $DW_{tot} = DW_{standing} + DW_{down}$ ). **(issue #44-but just delete  
193 this chunk if not resolved before submission)** Henceforth, we refer to the variables on the left side of  
194 the equation as “aggregate” fluxes or stocks, and those that are summed as “component” fluxes or stocks,  
195 noting that the same variable can take both aggregate and component positions in different relationships.  
196 We considered the C budget for a given relationship “closed” when component variables summed to within  
197 one standard deviation of the aggregate variable.

198 To test for differences across mature forest biomes, we also examined how stand age impacted fluxes and  
199 stocks, employing a mixed effects model [‘lmer’ function in ‘lme4’ R package version **x.xx; REF**] with biome  
200 as fixed effect and plot nested within geographic.area as random effects on the intercept. When Biome had a  
201 significant effect, we looked at a Tukey’s pairwise comparison to see which biomes were significantly different  
202 from one another. This analysis was run for variables with records for at least seven distinct geographic areas  
203 in more than one biome, excluding any biomes that failed this criteria (Table 1).

204 To test for age trends in young (<100yrs) forests, we employed a mixed effects model with biome and  
205  $\log_{10}[\text{stand.age}]$  as fixed effects and plot nested within geographic.area as a random effect on the intercept.  
206 This analysis was run for variables with records for at least three distinct geographic areas in more than one  
207 biome, excluding any biomes that failed this criteria (Table 1). When the effect of stand age was significant  
208 at  $p \leq 0.05$  and when each biome had records for stands of at least 10 different ages, a biome  $\times$  stand.age  
209 interaction was included in the model.

210 To facilitate the accessibility of our results and data, and to allow for rapid updates as additional data  
211 become available, we have automated all database manipulation, analyses, and figure production in R  
212 (**version, citation**).

## 213 Review Results/ Synthesis

### 214 Data Coverage

215 Of the 39762 records in *ForC* v3.0, 11923 met our strict criteria for inclusion in this study (Fig. 1). These  
216 records were distributed across 5062 plots in 865 distinct geographic areas. Of the 23 flux and 11 stock  
217 variables mapped in these diagrams, *ForC* contained sufficient mature forest data for inclusion in our  
218 statistical analyses (*i.e.*, records from  $\geq 7$  distinct geographic areas) for 20 fluxes and 9 stocks in tropical

219 broadleaf forests, 15 fluxes and 8 stocks in temperate broadleaf forests, 14 fluxes and 7 stocks in temperate  
220 conifer forests, and 8 fluxes and 7 stocks in boreal forests. For regrowth forests (<100 yrs), *ForC* contained  
221 sufficient data for inclusion in our statistical analyses (*i.e.*, records from  $\geq 3$  distinct geographic areas) for 11  
222 fluxes and 10 stocks in tropical broadleaf forests, 16 fluxes and 10 stocks in temperate broadleaf forests, 16  
223 fluxes and 10 stocks in temperate conifer forests, and 14 fluxes and 9 stocks in boreal forests.

224 **C cycling in mature forests**

225 Average C cycles for mature tropical broadleaf, temperate broadleaf, temperate conifer, and boreal forests  $\geq$   
226 100 years old and with no known major natural or anthropogenic disturbance are presented in Figures 2-5  
227 (and available in tabular format in the *ForC* release accompanying this publication:

228 [ForC/numbers\\_and\\_facts/ForC\\_variable\\_averages\\_per\\_Biome.csv](#)).

229 For variables with records from  $\geq 7$  distinct geographic areas, these ensemble C budgets were generally  
230 consistent. That is, component variables summed to within one standard deviation of their respective  
231 aggregate variables in all but one instance. In the temperate conifer biome, the average composite measure of  
232 root biomass ( $B_{root}$ ) was less than the combined average value of coarse and fine root biomass ( $B_{root-coarse}$   
233 and  $B_{root-fine}$ , respectively). This lack of closure was driven by very high estimates of  $B_{root-coarse}$  from  
234 high-biomass forests of the US Pacific Northwest.



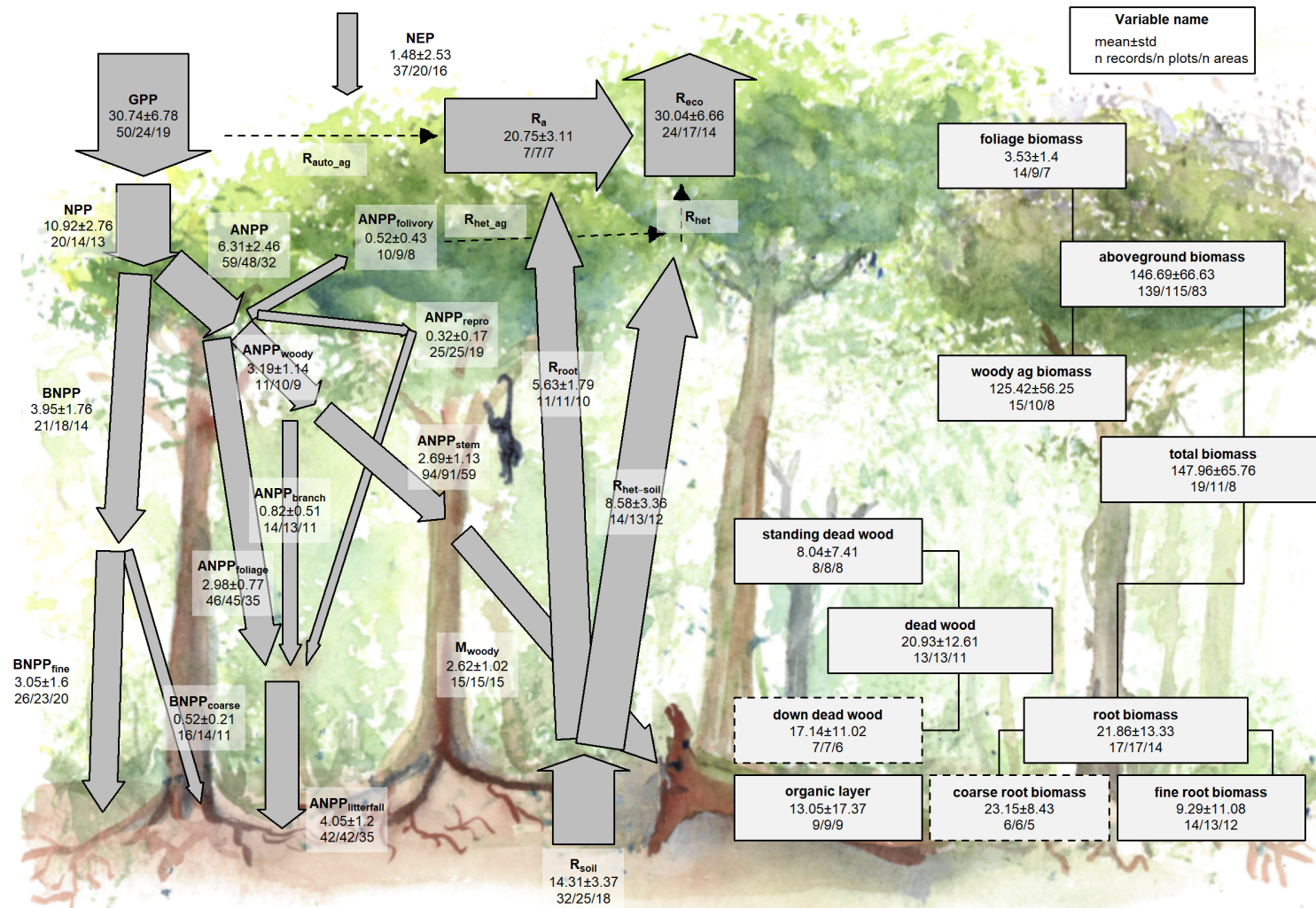


Figure 2 | C cycle diagram for mature tropical broadleaf forests. Arrows indicate fluxes ( $\text{Mg C ha}^{-1} \text{ yr}^{-1}$ ); boxes indicate stocks ( $\text{Mg C ha}^{-1}$ ), with variables as defined in Table 1. Presented are mean  $\pm$  std, where geographically distinct areas are treated as the unit of replication. Dashed shape outlines indicate variables with records from  $<7$  distinct geographic areas, and dashed arrows indicate fluxes with no data. To illustrate the magnitude of different fluxes, arrow size is proportional to the square root of corresponding flux. Asterisk after variable name indicates lack of C cycle closure.

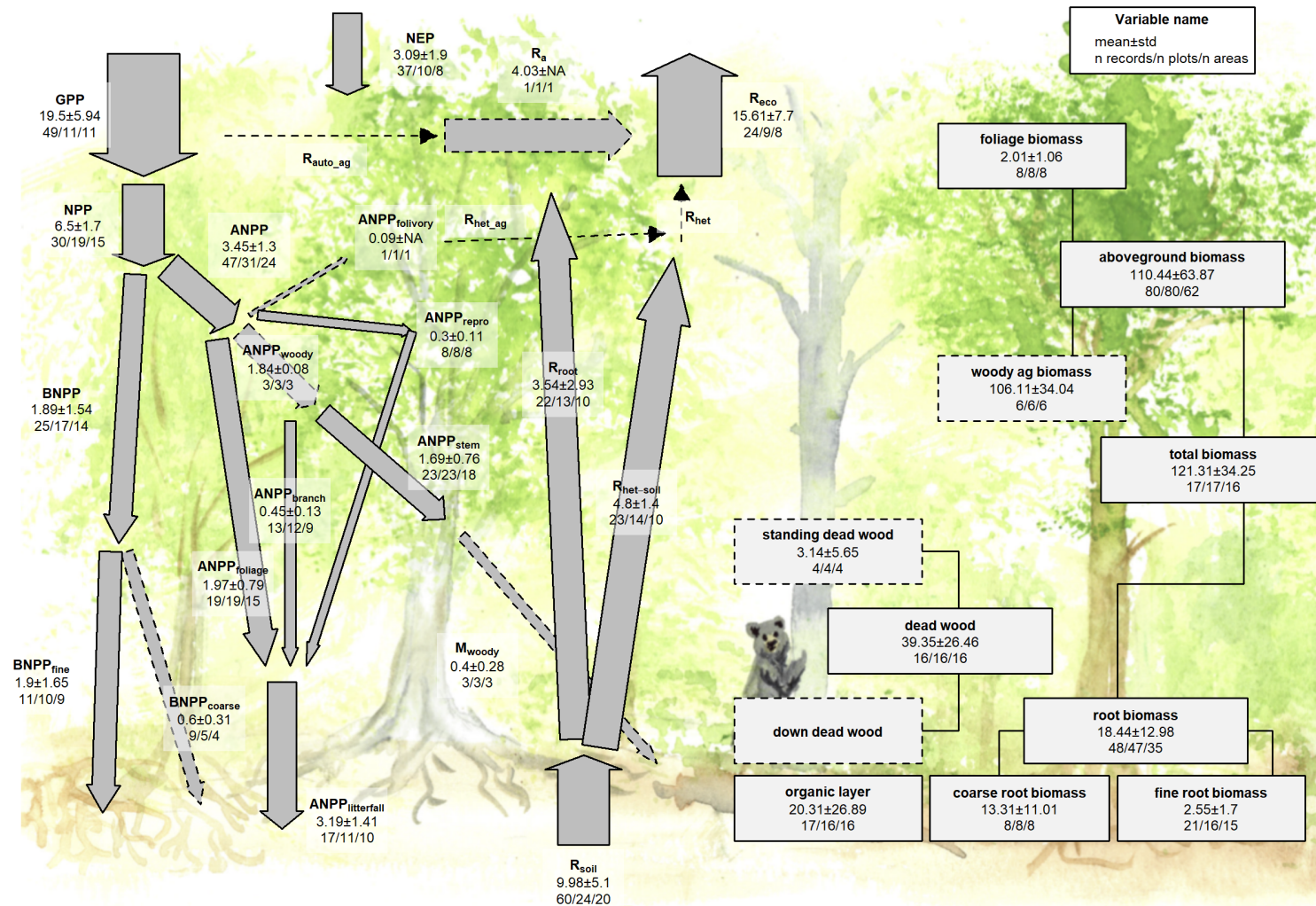


Figure 3 | C cycle diagram for mature temperate broadleaf forests. Arrows indicate fluxes ( $\text{Mg C ha}^{-1} \text{ yr}^{-1}$ ); boxes indicate stocks ( $\text{Mg C ha}^{-1}$ ), with variables as defined in Table 1. Presented are mean  $\pm$  std, where geographically distinct areas are treated as the unit of replication. Dashed shape outlines indicate variables with records from <7 distinct geographic areas, and dashed arrows indicate fluxes with no data. To illustrate the magnitude of different fluxes, arrow size is proportional to the square root of corresponding flux. Asterisk after variable name indicates lack of C cycle closure.

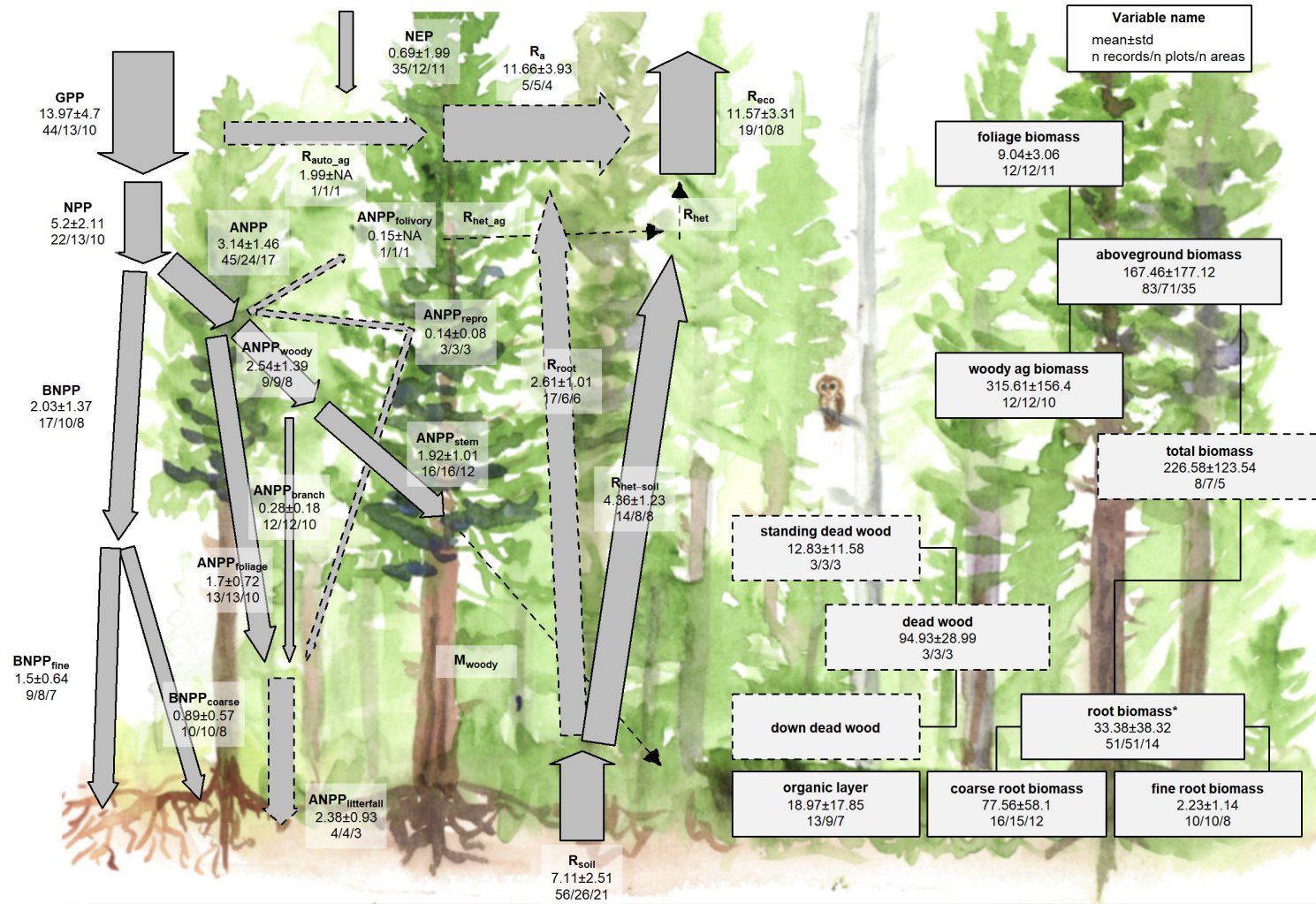


Figure 4 | C cycle diagram for mature temperate conifer forests. Arrows indicate fluxes ( $\text{Mg C ha}^{-1} \text{ yr}^{-1}$ ); boxes indicate stocks ( $\text{Mg C ha}^{-1}$ ), with variables as defined in Table 1. Presented are mean  $\pm$  std, where geographically distinct areas are treated as the unit of replication. Dashed shape outlines indicate variables with records from  $<7$  distinct geographic areas, and dashed arrows indicate fluxes with no data. To illustrate the magnitude of different fluxes, arrow size is proportional to the square root of corresponding flux. Asterisk after variable name indicates lack of C cycle closure.

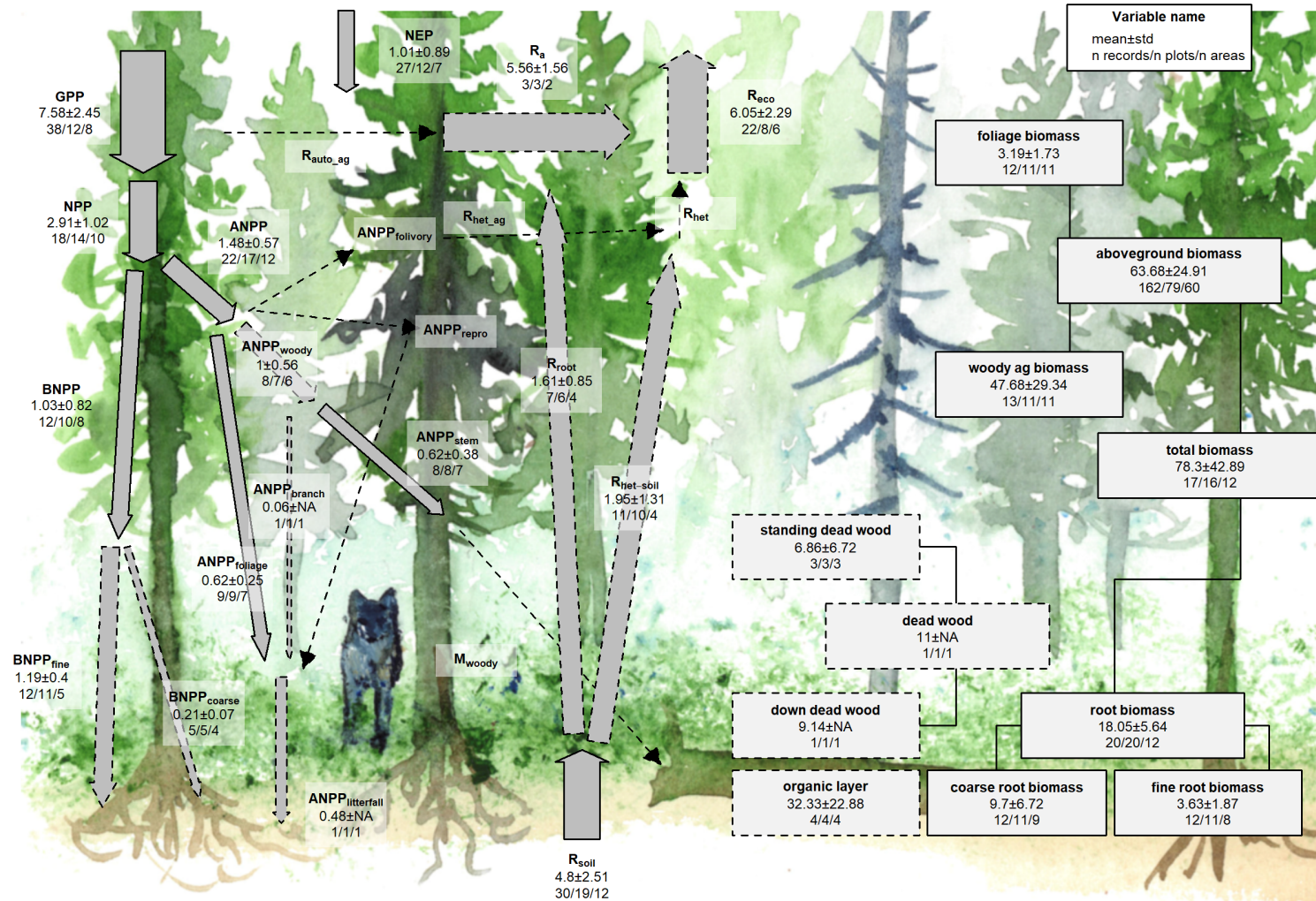


Figure 5 | C cycle diagram for mature boreal conifer forests. Arrows indicate fluxes ( $\text{Mg C ha}^{-1} \text{ yr}^{-1}$ ); boxes indicate stocks ( $\text{Mg C ha}^{-1}$ ), with variables as defined in Table 1. Presented are mean  $\pm$  std, where geographically distinct areas are treated as the unit of replication. Dashed shape outlines indicate variables with records from  $<7$  distinct geographic areas, and dashed arrows indicate fluxes with no data. To illustrate the magnitude of different fluxes, arrow size is proportional to the square root of corresponding flux. Asterisk after variable name indicates lack of C cycle closure.

235 There were sufficient data to assess mature forest biome differences for 15 flux variables, and significant  
236 differences among biomes were detected for 12 variables (Table 1). In all of these cases—including C fluxes  
237 into, within, and out of the ecosystem—C fluxes were highest in tropical forests, intermediate in temperate  
238 (broadleaf or conifer) forests, and lowest in boreal forests (Table 1, Figs. 6, S1-S15). Differences between  
239 tropical and boreal forests were always significant, with temperate forests intermediate and significantly  
240 different from one or both. Fluxes tended to be numerically greater in temperate broadleaf than conifer  
241 forests, but the difference was never statistically significant. This pattern held for the following variables:  
242  $GPP\$$ ,  $NPP$ ,  $ANPP$ ,  $ANPP_{stem}$ ,  $ANPP_{branch}$ ,  $ANPP_{foliage}$ ,  $BNPP$ ,  $R_{eco}$ ,  $R_{root}$ ,  $R_{soil}$ , and  $R_{het-soil}$ .  
243 For two of the variables without significant differences among biomes ( $ANPP_{litterfall}$  and  $BNPP_{fine}$ ; Figs.  
244 S8 and S11, respectively), the same general trends applied but were not statistically significant. Another  
245 exception was for  $BNPP_{root-coarse}$ , where all records came from high-biomass forests in the US Pacific  
246 Northwest, resulting in marginally higher values for the temperate conifer biome (Table 1, Fig. S10;  
247 differences significant in mixed effects model but not in post-hoc pairwise comparison).

248 The most notable exception to the pattern of decreasing flux from tropical to boreal biomes was  $NEP$ , with  
249 no significant differences across biomes but with the largest average in temperate broadleaf forests, followed  
250 by tropical, boreal, and temperate conifer forests (Figs. 5,S1).

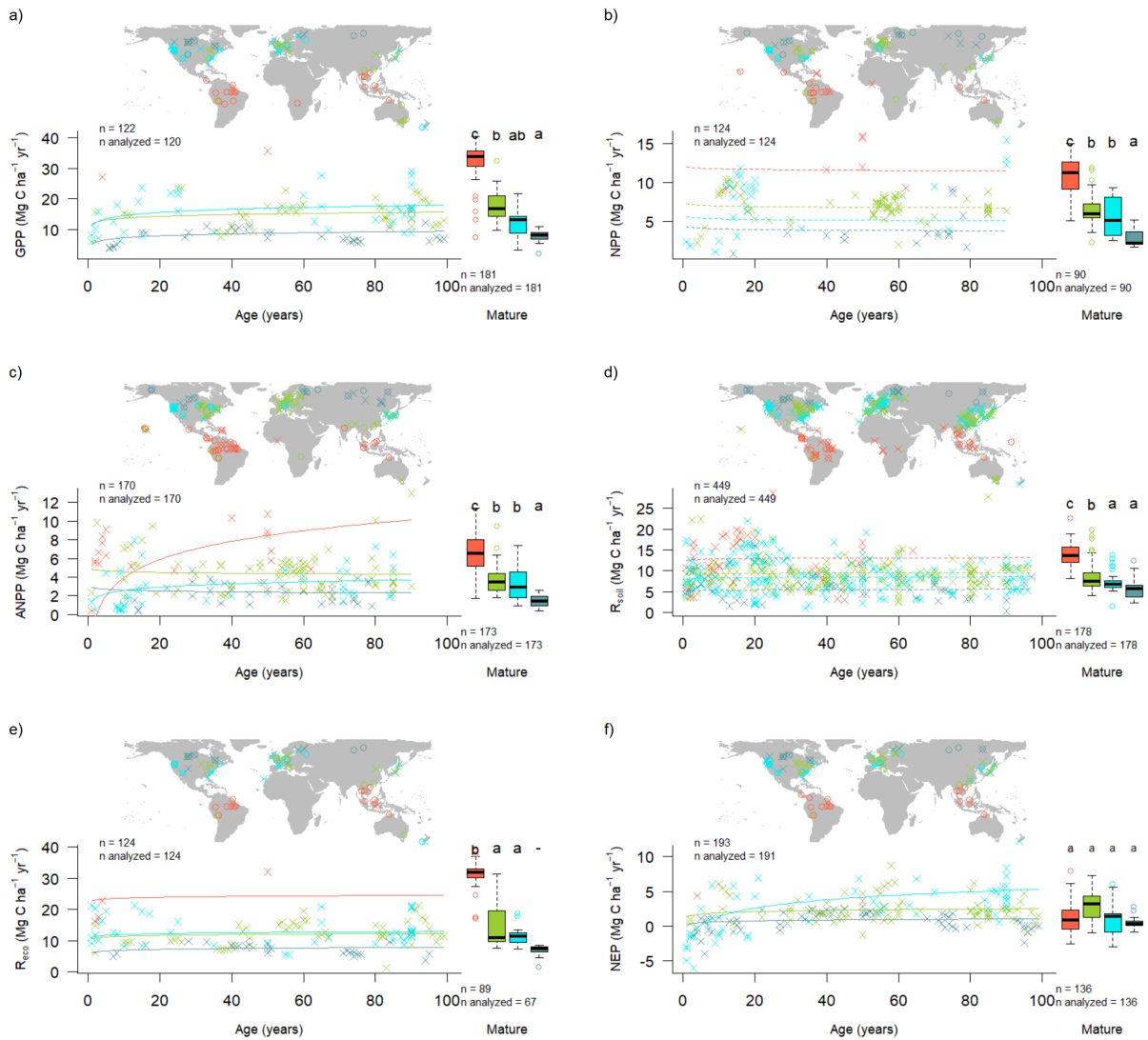


Figure 6 | Age trends and biome differences in some of the major C fluxes: (a)  $GPP$ , (b)  $NPP$ , (c)  $ANPP$ , (d)  $R_{\text{soil}}$ , (e)  $R_{\text{eco}}$ , and (f)  $NEP$ . Map shows data sources ( $x$  and  $o$  indicate young and mature stands, respectively). In each panel, the left scatterplot shows age trends in forests up to 100 years old, as characterized by a linear mixed effects model with fixed effects of age and biome. The fitted line indicates the effect of age on flux (solid lines: significant at  $p < 0.05$ , dashed lines: non-significant), and non-parallel lines indicate a significant age  $\times$  biome interaction. The boxplot illustrates distribution across mature forests, with different letters indicating significant differences between biomes. Data from biomes that did not meet the sample size criteria (see Methods) are plotted, but lack regression lines (young forests) or test of differences across biomes (mature forests). Individual figures for each flux with sufficient data are given in the Supplement (Figs. S1-S15).

251 There were sufficient data to assess mature forest biome differences for nine stock variables, and significant  
 252 differences among biomes were detected for five variables ( $B_{\text{tot}}$ ,  $B_{\text{ag}}$ ,  $B_{\text{ag-wood}}$ ,  $B_{\text{foliage}}$ ,  $B_{\text{root-coarse}}$ ; Table  
 253 1). C stocks had less consistent patterns across biomes (Figs. 7, S16-S26). For  $B_{\text{tot}}$  and  $B_{\text{ag}}$ , tropical  
 254 broadleaf forests had the highest biomass and boreal forests the lowest, with temperate broadleaf and  
 255 needleleaf ( $B_{\text{ag}}$  only) intermediate. For three variables that had been disproportionately sampled in the  
 256 high-biomass forests of the US Pacific Northwest ( $B_{\text{ag-wood}}$ ,  $B_{\text{foliage}}$ , and  $B_{\text{root-coarse}}$ ), temperate conifer  
 257 forests had significantly higher stocks than the other biomes, which were not significantly different from one  
 258 another.

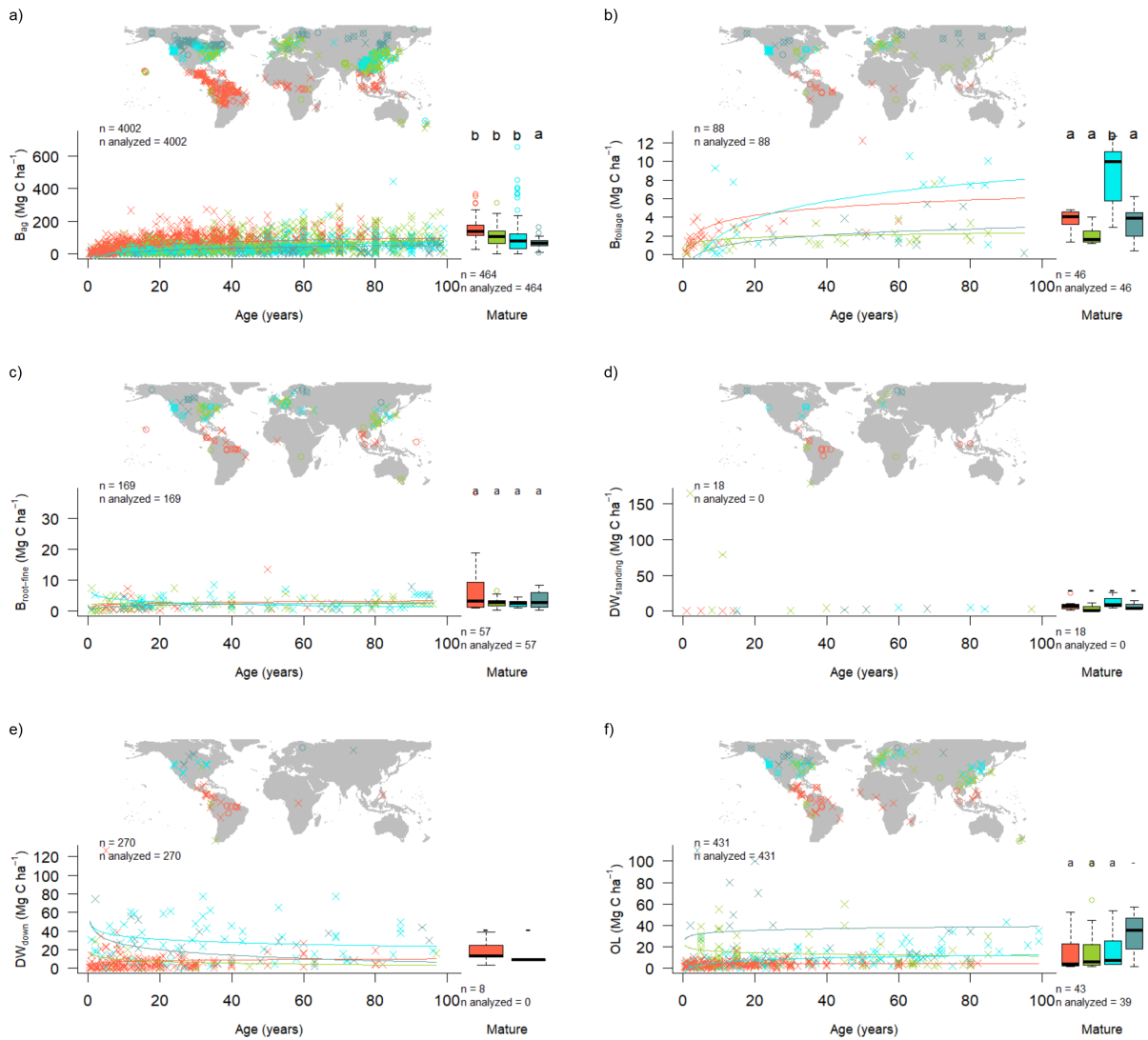


Figure 7 | Age trends and biome differences in some of the major forest C stocks: (a) aboveground biomass, (b) foliage, (c) fine roots, (d) dead wood. Map shows data sources ( $x$  and  $o$  indicate young and mature stands, respectively). In each panel, the left scatterplot shows age trends in forests up to 100 years old, as characterized by a linear mixed effects model with fixed effects of age and biome. The fitted line indicates the effect of age on flux (solid lines: significant at  $p < 0.05$ , dashed lines: non-significant), and non-parallel lines indicate a significant age  $\times$  biome interaction. The boxplot illustrates distribution across mature forests, with different letters indicating significant differences between biomes. Data from biomes that did not meet the sample size criteria (see Methods) are plotted, but lack regression lines (young forests) or test of differences across biomes (mature forests). Individual figures for each stock with sufficient data are given in the Supplement (Figs. S16-S26).

## 259 C cycling in young forests

260 Average C cycles for forests  $<100$  years old are presented in Figures 8-11.  
 261 Both C stocks and fluxes commonly increased significantly with stand age (Tables 1, S2, Figs. 6-11, S1-S26;  
 262 detailed below).

263 ForC contained 16 C flux variables with sufficient data for analyses of age trends in young forests (see  
 264 Methods) (Figs. 6, S1-S15). Of these, ten increased significantly with age:  $NEP$ ,  $GPP$ ,  $ANPP$ ,  
 265  $ANPP_{woody}$ ,  $ANPP_{foliage}$ ,  $ANPP_{litterfall}$ ,  $BNPP$ ,  $BNPP_{fine}$ ,  $R_{eco}$ , and  $R_{root}$ . The remaining six— $NPP$ ,

- 266  $ANPP_{stem}$ ,  $ANPP_{branch}$ ,  $BNPP_{coarse}$ ,  $R_{soil-het}$ , and  $R_{soil-het}$ -displayed no significant relationship to  
267 stand age.
- 268 Differences in C fluxes across biomes typically paralleled those observed for mature forests, with C cycling  
269 generally most rapid in the tropics and slowest in boreal forests.
- 270 The single exception was  $ANPP_{stem}$ , for which temperate broadleaf and conifer forests had similar flux rates  
271 than tropical forests. Notably, and in contrast to the lack of biome differences in  $NEP$  for mature forests  
272 (Fig. 6), the tendency for temperate forests to have greater fluxes than boreal forests held for  $NEP$  in  
273 regrowth forests (tropical forests excluded because of insufficient data).
- 274 In terms of C stocks, ten variables (all but standing deadwood,  $DW_{standing}$ ) had sufficient data to test for  
275 age trends (Table 1, Figs. 7, S16-26). All of these increased significantly with  $\log_{10}[stand.age]$ . There were  
276 sufficient data to model age x biome interactions were also significant for all ten of these C stock variables  
277 (Table S2). (**return here after Valentine checks whether differences in Table 1 were significant!** )
- 278 In the case of two non-living C stocks ( $DW_{down}$  and  $OL$ )



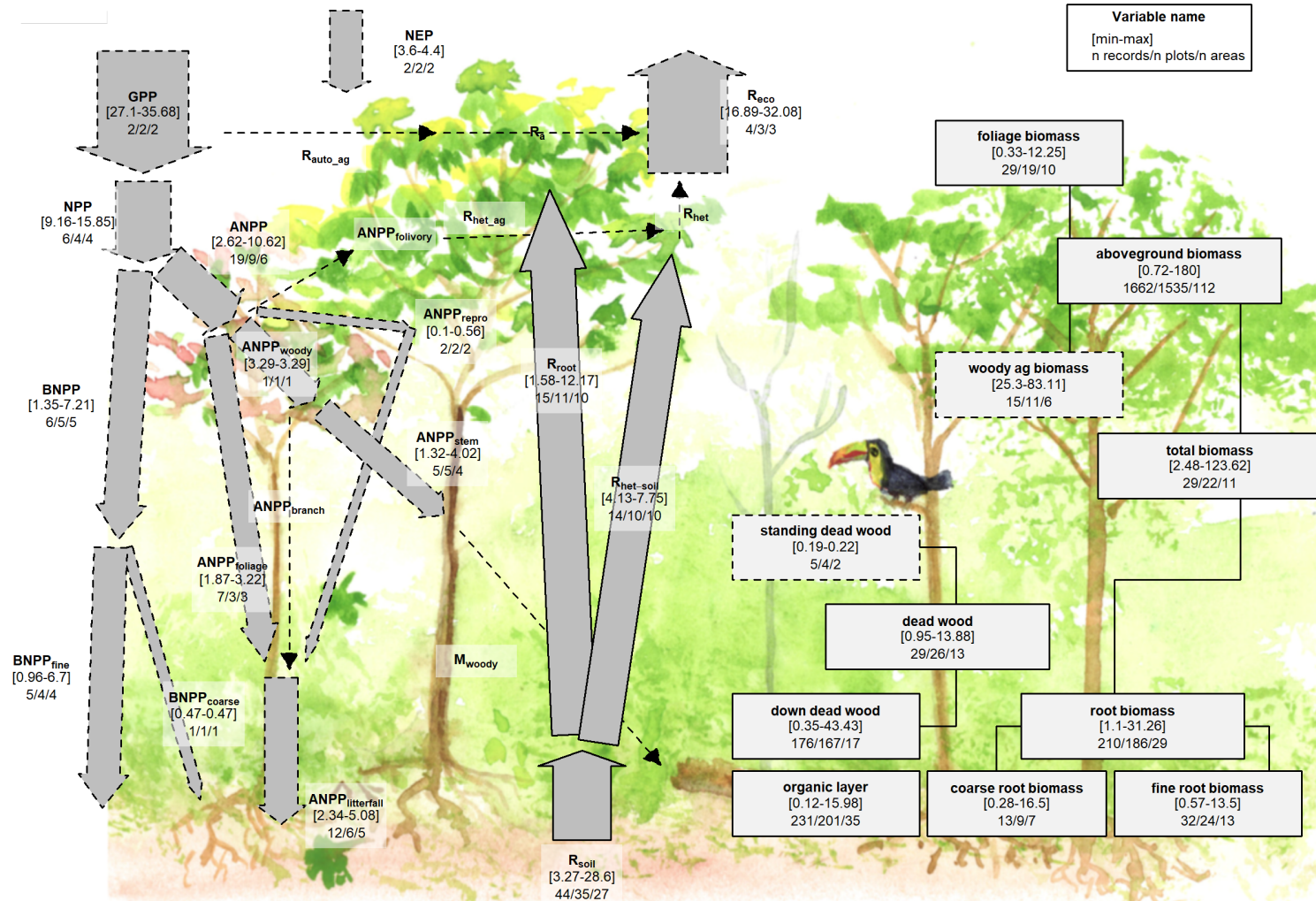


Figure 8 | C cycle diagram for young tropical broadleaf forests. Arrows indicate fluxes ( $\text{Mg C ha}^{-1} \text{ yr}^{-1}$ ); boxes indicate stocks ( $\text{Mg C ha}^{-1}$ ), with variables as defined in Table 1. Presented are observed ranges, where geographically distinct areas are treated as the unit of replication. All units are  $\text{Mg C ha}^{-1} \text{ yr}^{-1}$  (fluxes) or  $\text{Mg C ha}^{-1}$  (stocks). Dashed shape outlines indicate variables with records from <7 distinct geographic areas, and dashed arrows indicate fluxes with no data. To illustrate the magnitude of different fluxes, arrow size is proportional to the square root of corresponding flux.

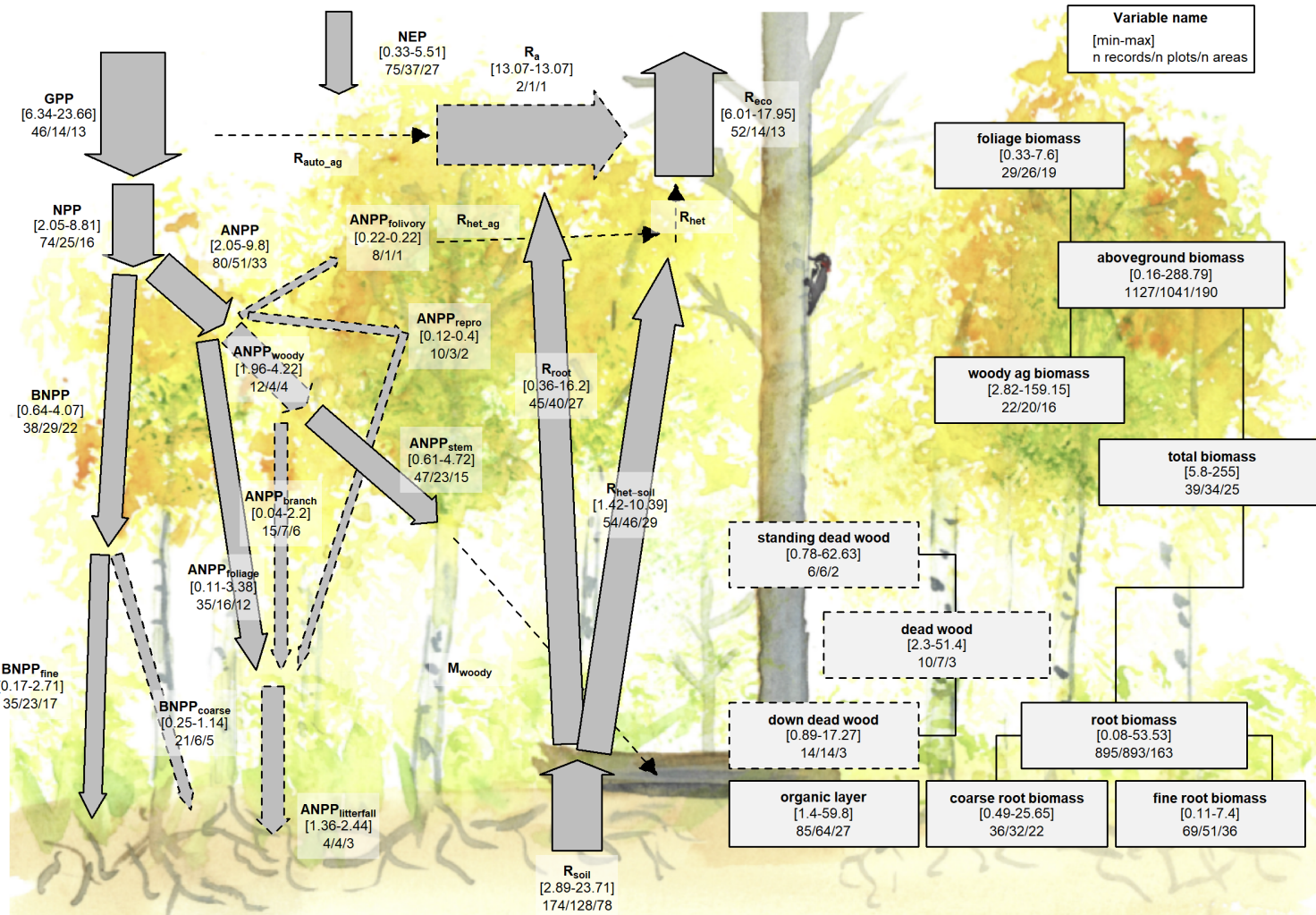


Figure 9 | C cycle diagram for young temperate broadleaf forests. Arrows indicate fluxes ( $\text{Mg C ha}^{-1} \text{ yr}^{-1}$ ); boxes indicate stocks ( $\text{Mg C ha}^{-1}$ ), with variables as defined in Table 1. Presented are observed ranges, where geographically distinct areas are treated as the unit of replication. All units are  $\text{Mg C ha}^{-1} \text{ yr}^{-1}$  (fluxes) or  $\text{Mg C ha}^{-1}$  (stocks). Dashed shape outlines indicate variables with records from <7 distinct geographic areas, and dashed arrows indicate fluxes with no data. To illustrate the magnitude of different fluxes, arrow size is proportional to the square root of corresponding flux.

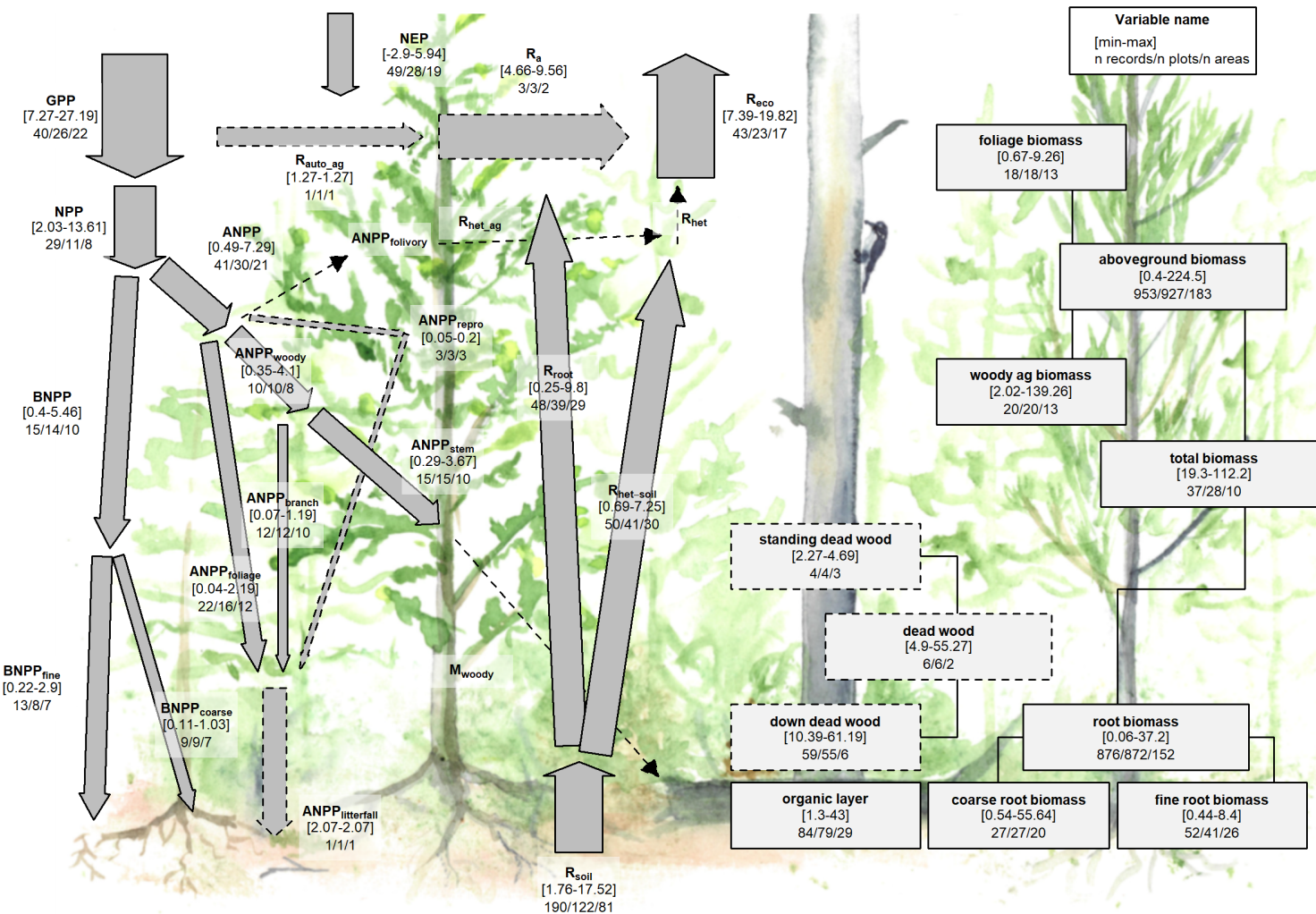


Figure 10 | C cycle diagram for young temperate conifer forests. Arrows indicate fluxes ( $\text{Mg C ha}^{-1} \text{ yr}^{-1}$ ); boxes indicate stocks ( $\text{Mg C ha}^{-1}$ ), with variables as defined in Table 1. Presented are observed ranges, where geographically distinct areas are treated as the unit of replication. All units are  $\text{Mg C ha}^{-1} \text{ yr}^{-1}$  (fluxes) or  $\text{Mg C ha}^{-1}$  (stocks). Dashed shape outlines indicate variables with records from <7 distinct geographic areas, and dashed arrows indicate fluxes with no data. To illustrate the magnitude of different fluxes, arrow size is proportional to the square root of corresponding flux.

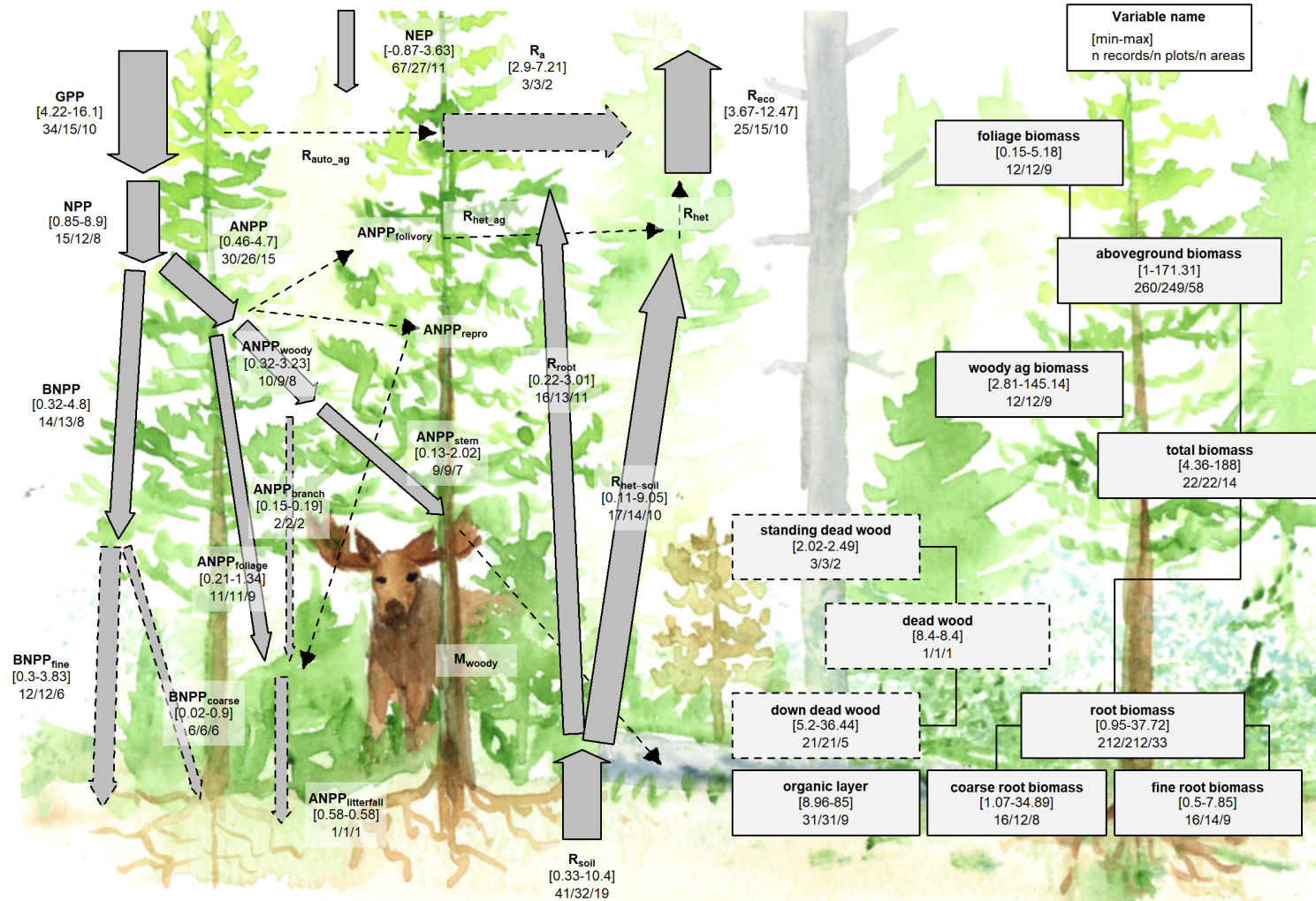


Figure 11 | C cycle diagram for young boreal conifer forests. Arrows indicate fluxes ( $Mg\ C\ ha^{-1}\ yr^{-1}$ ); boxes indicate stocks ( $Mg\ C\ ha^{-1}$ ), with variables as defined in Table 1. Presented are observed ranges, where geographically distinct areas are treated as the unit of replication. All units are  $Mg\ C\ ha^{-1}\ yr^{-1}$  (fluxes) or  $Mg\ C\ ha^{-1}$  (stocks). Dashed shape outlines indicate variables with records from <7 distinct geographic areas, and dashed arrows indicate fluxes with no data. To illustrate the magnitude of different fluxes, arrow size is proportional to the square root of corresponding flux.

279 **Discussion**

280 *ForC* v3.0 provided unprecedented coverage of most major variables, yielding an internally consistent picture  
281 of C cycling in the world's major forest biomes. Carbon cycling rates generally increased from boreal to  
282 tropical regions and with stand age. Specifically, the major C fluxes were highest in tropical forests,  
283 intermediate in temperate (broadleaf or conifer) forests, and lowest in boreal forests – a pattern that generally  
284 held for regrowth as well as mature forests (Figs. 6-7). In contrast to C fluxes, there was little directional  
285 variation in mature forest C stocks across biomes (Figs. 2-5, 7). The majority of flux variables, together with  
286 most live biomass pools, increased significantly with stand age (Figs. 6-11). Together, these results indicate  
287 that, moving from cold to tropical climates and from young to old stands, there is a general acceleration of C  
288 cycling, whereas C stocks and *NEP* of mature forests are correlated with a different set of factors.

289 **C variable coverage and budget closure**

290 The large number of C cycle variables covered by *ForC*, and the general consistency between them, provide  
291 confidence that our overall reported means provide accurate and useful baselines for analysis (with the  
292 caveats that they are unlikely to be accurate representations of C cycling for any particular forest, and that  
293 these sample means almost certainly do not represent true biome means).

294 There are of course notable holes in the *ForC* variable coverage, as discussed by Anderson-Teixeira et  
295 al. (xxxx), that limit the scope of our inferences here. Notably, *ForC* lacks coverage of fluxes to herbivores  
296 and higher consumers, along with the woody mortality and dead wood stocks. Geographically, all variables  
297 are poorly covered in Africa and Siberia, a common problem in the carbon-cycle community (Xu and Shang  
298 2016 10.1016/j.jplph.2016.08.007, Schimel et al. 2015 10.1073/pnas.1407302112). *ForC* does not include soil  
299 carbon, which is covered by other efforts (e.g. Köchy et al. 2015 10.5194/soil-1-351-2015). *ForC* is not  
300 intended to replace databases that are specialized for particular parts of the C cycle analyses, e.g.,  
301 aboveground biomass (REFS), land-atmosphere fluxes (Baldocchi et al. 2001  
302 10.1175/1520-0477(2001)082<2415:FANTTS>2.3.CO;2), soil respiration (Jian et al. 2020  
303 10.5194/essd-2020-136), or the human footprint in global forests (Magnani et al. 2007 10.1038/nature05847).

304 In this analysis, the C cycle budgets for mature forests (Figs. 2-5) generally “close”—that is, the sums of  
305 component variables do not differ from the larger fluxes by more than one standard deviation. On the one  
306 hand, this reflects the general fact that ecosystem-scale measurements tend to close the C budget more easily  
307 and consistently than, for example, for energy balance (Stoy et al. 2013 10.1016/j.agrformet.2012.11.004). On  
308 the other, however, as noted above *ForC* derives data from multiple heterogeneous sources, often with large  
309 errors (standard deviations); as a result, the standard for C closure is relatively loose (cf Houghton 2020  
310 10.1111/gcb.15050). Nonetheless, the lack of closure, in the few instances where it occurs, is probably more  
311 reflective of differences in the representation of forest types (e.g., disproportionate representation of US  
312 Pacific NW for aboveground woody biomass relative to AGB; Fig. 4) than of methodological accuracy. The  
313 overall high degree of closure implies that *ForC* gives a consistent picture of C cycling within biomes. This is  
314 an important and useful test, because it allows for consistency checks within the C cycle, for example  
315 leveraging separate and independently-measured fluxes to constrain errors in another (Phillips et al. 2017  
316 10.1007/s11104-016-3084-x, Williams et al. 2014 10.1016/j.rse.2013.10.034, Harmon et al. 2011  
317 10.1029/2010JG001495), or producing internally consistent global data products (Wang et al. 2018  
318 10.5194/gmd-11-3903-2018).

319 **C cycling across biomes**

320 Our analysis reveals a general deceleration of carbon cycling from the tropics to boreal regions. For mature  
321 forests, this is consistent with a large body of previous work demonstrating that C fluxes generally decline  
322 with latitude (or increase with temperature) on a global scale (e.g., ???, ???, Li and Xiao 2019, Banbury  
323 Morgan *et al* n.d.). The consistency with which this occurs across numerous fluxes is not surprising, but has  
324 never been simultaneously assessed across such a large number of variables (but see Banbury Morgan *et al*  
325 n.d. for nine autotrophic fluxes). Thus, our analysis reveals that carbon cycling is most rapid in the tropics  
326 and slowest in boreal regions, including C fluxes into (*GPP*), within (e.g., *NPP* and its components), and  
327 out of (e.g.,  $R_{soil}$ ,  $R_{eco}$ ) the ecosystem.

328 The notable exception to the pattern of fluxes decreasing from tropical to boreal regions is *NEP* (Fig. 6f),  
329 which showed no significant differences across biomes. Unlike the other C flux variables, *NEP* does not  
330 represent the rapidity with which C cycles through the ecosystem, but is the balance between C  
331 sequestration (*GPP*) and respiratory losses ( $R_{eco}$ ) and represents net CO<sub>2</sub> sequestration (or release) by the  
332 ecosystem. *NEP* tends to be relatively small in mature forest stands [(???)**, MORE REFS?**; discussed  
333 further below], which accumulate carbon slowly relative to younger stands [(???)**; REFS**], if at all (**REFS**).  
334 It is therefore unsurprising that there are no pronounced differences across biomes, suggesting that variation  
335 in *NEP* of mature forests is controlled less by climate and more by other factors including moderate  
336 disturbances (**REFS**) or disequilibrium of  $R_{soil}$  relative to C inputs [e.g., in peatlands where anoxic  
337 conditions inhibit decomposition; **REFS**].

338 In contrast to the patterns observed for *NEP* in mature stands, *NEP* of stands between 20 and 100 years of  
339 age varied across biomes, being lowest in boreal forests, intermediate in temperate broadleaf forests, and  
340 highest in temperate conifer forests (with insufficient data to assess tropical forests; Figs. 6f, S1). This is  
341 consistent with findings that live biomass accumulation rates (e.g.,  $\Delta B_{ag}$  or  $\Delta B_{tot}$ ) during early secondary  
342 succession decrease with latitude [Anderson *et al* (2006); Cook-Patton *et al* (2020); Figs. 7a, S16-S22]. Note,  
343 though, that *NEP* includes not only  $\Delta B_{tot}$ , but also changes in *DW<sub>tot</sub>*, *OL*, and soil carbon, and biome  
344 differences in the accumulation rates of these variables have not been detected, in part because these variables  
345 do not consistently increase with stand age [Cook-Patton *et al* (2020); Figs. 7, S23-S26; see discussion below].

346 For regrowth forests, little is known about cross-biome differences in carbon fluxes, and we are not aware of  
347 any previous large-scale comparisons of C fluxes that have been limited to regrowth forests [although they're  
348 commonly mixed in with mature forests; e.g., **REFS**]. Thus, this analysis was the first to examine flux  
349 trends in regrowth forests across biomes. The observed tendency for young forest fluxes to decrease from  
350 tropical to boreal regions paralleled patterns in mature forests (Figs. 6, S1-S15), suggesting that regrowth  
351 forests follow latitudinal trends in carbon cycling similar to those of mature forests (e.g., Banbury Morgan *et*  
352 *al* n.d.). Yet, *data remain sparse, and further work will be required to explore age x climate*  
353 *interactions. Nevertheless, our broad-brush overview indicates that C cycling of regrowth forests is not only*  
354 *higher in the tropics, parallel to fluxes in mature forests (Banbury Morgan et al n.d.), but also that it*  
355 *accelerates more rapidly with stand age in the tropics, consistent with more rapid biomass accumulation.*

356 In contrast to C fluxes and biomass accumulation rates in regrowth forests, stocks showed less systematic  
357 variation across biomes. For aboveground biomass, this Patterns are consistent with others studies showing  
358 that variation in forest biomass across broad climatic gradients is modest and constrained more by moisture  
359 than temperature (???)**. (???)**, using spaceborne lidar, showed a decline in aboveground biomass (all forests,

360 including secondary) with latitude in the N hemisphere, but values exceeding tropical forests in coastal  
361 climates of both the southern and northern hemisphere. Highest biomass forests are found in temperate  
362 oceanic climates (REF- , something in GEB, some global forest C map) (???). Lack of synthesis comparing  
363 deadwood and organic layer across biomes, but see Cook-Patton *et al* (2020) for age trends.

364 Thus, biome differences should be interpreted more as driven more by geographic distribution of sampling  
365 than by true differences.

### 366 Age trends in C cycling

367 (*Just some rough notes at this point*)

368 A relative dearth of data on C cycling in secondary forests, particularly in the tropics (Anderson-Teixeira et  
369 al 2016), is problematic in that almost 2/3 of the world's forests were secondary as of 2010 (FAO 2010),  
370 implying an under-filled need to characterize age-related trends in forest C cycling.

371 Moreover, as disturbances increase (???, McDowell *et al* 2020), understanding the carbon dynamics of  
372 regrowth forests will be increasingly important.

373 It's also important to understand secondary forest C sequestration to reduce uncertainty regarding the  
374 potential for carbon uptake by regrowth forests (???, Cook-Patton *et al* 2020).

375 (discuss NEP well, including) NEP increases with log(age) to 100 -> strongest C sinks are established  
376 secondary forests. (But presumably this exact number is an artifact; don't over-emphasize.)

377 Our findings are largely consistent with, but built from a far larger dataset than, those of Pregitzer and  
378 Euskirchen (2004 <http://dx.doi.org/10.1111/j.1365-2486.2004.00866.x>), who found that NPP and NEP to be  
379 higher in intermediate-aged forests than older forests, and emphasize the importance of forest age at the  
380 biome scale. Quickly-changing and age-dependent fluxes were also found in a number of previous syntheses  
381 (Amiro et al. 2010 10.1029/2010JG001390, Magnani et al. 2007 10.1038/nature05847).

382 In contrast to most fluxes, *NEP* is highest at intermediate ages

### 383 Relevance for climate change prediction and mitigation

384 The future of forest C cycling (???) will shape trends in atmospheric CO<sub>2</sub> and the course of climate change.  
385 For a human society seeking to understand and mitigate climate change, the data contained in *ForC* and  
386 summarized here can help to meet two major challenges.

387 First, improved representation of forest C cycling in models is essential to improving predictions of the future  
388 course of climate change. To ensure that models are giving the right answers for the right reasons, it is  
389 important to benchmark against multiple components of the C cycle that are internally consistent with each  
390 other. By making tens of thousands of records readily available in standardized format, *ForC* makes it  
391 feasible for the modeling community to draw upon these data to benchmark models. Integration of *ForC*  
392 with models is a goal (Fer et al., in revision).

393 Second, *ForC* can serve as a pipeline through which forest science can inform forest-based climate change  
394 mitigation efforts. Such efforts will be most effective when informed by the best available data, yet it is not  
395 feasible for the individuals and organizations designing such efforts to sort through literature, often behind  
396 paywalls, with data reported in varying units, terminology, etc. One goal for *ForC* is to serve as a pipeline

397 through which information can flow efficiently from forest researchers to decision-makers working to  
398 implement forest conservation strategies at global, national, or landscape scales. This is already happening!  
399 *ForC* has already contributed to updating the IPCC guidelines for carbon accounting in forests [IPCC 2019;  
400 Requena Suarez *et al* (2019); Rozendaal *et al* in prep], mapping C accumulation potential from natural forest  
401 regrowth globally (Cook-Patton *et al* 2020), and informing ecosystem conservation priorities (Goldstein *et al*  
402 2020).

403 **ForC can complement remote sensing to provide a comprehensive picture of global forest C**  
404 **cycling.** (*here, discuss what is well-covered by remote sensing, where ForC is useful for calibrating remote*  
405 *sensing, and what ForC can get that remote sensing can't.*) AGB is the largest stock, and most of the  
406 emphasis is on this variable. Remote sensing, with calibration based on high-quality ground-based data  
407 (Schepaschenko *et al* 2019, Chave *et al* 2019), is the best approach for mapping forest carbon (REFS).  
408 However, it is limited in that it is not associated with stand age and disturbance history, except in recent  
409 decades when satellite data can be used to detect forest loss, gain, and some of their dominant drivers  
410 (Hansen *et al* 2013, Song *et al* 2018, Curtis *et al* 2018). *ForC* is therefore valuable in defining age-based  
411 trajectories in biomass, as in Cook-Patton *et al* (2020).

412 *Remote sensing measurements are increasingly useful for global- or regional-scale estimates of forest GPP*  
413 *(???, Li and Xiao 2019), aboveground biomass ( $B_{ag}$ ) (REFS), woody mortality (i.e.,  $B_{ag}$  losses to mortality*  
414  *$M_{woody}$ ) (Clark *et al* 2004, Leitold *et al* 2018), and to some extent net ecosystem exchange (NEP) (REFS).*  
415 Other variables, in particular respiration fluxes, cannot be remotely sensed ((??)), and efforts such as the  
416 Global Carbon Project (**le quere REF**) and NASA CMS (**citation:**  
417 [https://carbon.nasa.gov/pdfs/CMS\\_Phase-1\\_Report\\_Final\\_optimized.pdf](https://carbon.nasa.gov/pdfs/CMS_Phase-1_Report_Final_optimized.pdf) but maybe  
418 better to cite open literature, one of the papers listed at  
419 <https://cmsflux.jpl.nasa.gov/get-data/publication-data-sets>) typically compute them as residuals  
420 only. (**Ben, it woudl be particularly helpful if you could flesh this out some more.**)

421 In terms of C stocks, there is a paucity of data on dead wood and organic layer (Pan *et al.* ?). These can be  
422 significant. (**Note that we've given a lot of emphasis to dead wood (work by Abby), and as a**  
423 **result this work really advances knowledge of dead wood. We'll want to highlight that here.**)  
424 (*give some stats/ cite figures*).

425 **Move to data availability statement, or methods?:** We recommend that use of *ForC* data go to the  
426 original database, as opposed to using “off-the-shelf” values from this publication. This is because (1) *ForC*  
427 is constantly being updated, (2) analyses should be designed to match the application, (3) age equations  
428 presented here all fit a single functional form that is not necessarily the best possible for all the variables.  
429 As climate change accelerates, understanding and managing the carbon dynamics of forests will be critical to  
430 forecasting, mitigation, and adaptation. The C data in *ForC*, as summarized here, will be valuable to these  
431 efforts.

## 432 Acknowledgements

433 Thanks to all researchers whose data are included in *ForC* and this analysis, to Jennifer McGarvey and Ian  
434 McGregor for help with the database, and to Norbert Kunert for helpful discussion. Funding sources  
435 included a Smithsonian Scholarly Studies grant to KAT and HML and a Smithsonian Working Land and  
436 Seascapes grant to KAT.

437 **Data availability statement**

438 Materials required to fully reproduce these analyses, including data, R scripts, and image files, are archived  
439 in Zenodo (DOI: TBD]. Data, scripts, and results presented here are also available through the open-access  
440 *ForC* GitHub repository (<https://github.com/forc-db/ForC>), where many will be updated as the database  
441 develops.

442 **ORCID iD**

443 Kristina J. Anderson-Teixeira: <https://orcid.org/0000-0001-8461-9713>

444 **References**

- 445 Anderson K J, Allen A P, Gillooly J F and Brown J H 2006 Temperature-dependence of biomass  
446 accumulation rates during secondary succession *Ecology Letters* **9** 673–82 Online:  
447 <http://www.blackwell-synergy.com/doi/abs/10.1111/j.1461-0248.2006.00914.x>
- 448 Anderson-Teixeira K, Herrmann V, CookPatton, Ferson A and Lister K 2020 Forc-db/GROA: Release with  
449 Cook-Patton et al. 2020, Nature. Online: <https://zenodo.org/record/3983644>
- 450 Anderson-Teixeira K J, Davies S J, Bennett A C, Gonzalez-Akre E B, Muller-Landau H C, Joseph Wright S,  
451 Abu Salim K, Almeyda Zambrano A M, Alonso A, Baltzer J L, Basset Y, Bourg N A, Broadbent E N,  
452 Brockelman W Y, Bunyavejchewin S, Burslem D F R P, Butt N, Cao M, Cardenas D, Chuyong G B, Clay K,  
453 Cordell S, Dattaraja H S, Deng X, Detto M, Du X, Duque A, Erikson D L, Ewango C E N, Fischer G A,  
454 Fletcher C, Foster R B, Giardina C P, Gilbert G S, Gunatilleke N, Gunatilleke S, Hao Z, Hargrove W W,  
455 Hart T B, Hau B C H, He F, Hoffman F M, Howe R W, Hubbell S P, Inman-Narahari F M, Jansen P A,  
456 Jiang M, Johnson D J, Kanzaki M, Kassim A R, Kenfack D, Kibet S, Kinnaird M F, Korte L, Kral K,  
457 Kumar J, Larson A J, Li Y, Li X, Liu S, Lum S K Y, Lutz J A, Ma K, Maddalena D M, Makana J-R, Malhi  
458 Y, Marthews T, Mat Serudin R, McMahon S M, McShea W J, Memiaghe H R, Mi X, Mizuno T, Morecroft  
459 M, Myers J A, Novotny V, Oliveira A A de, Ong P S, Orwig D A, Ostertag R, Ouden J den, Parker G G,  
460 Phillips R P, Sack L, Sainge M N, Sang W, Sri-ngernyuang K, Sukumar R, Sun I-F, Sungpalee W, Suresh H  
461 S, Tan S, Thomas S C, Thomas D W, Thompson J, Turner B L, Uriarte M, Valencia R, et al 2015  
462 CTFS-ForestGEO: A worldwide network monitoring forests in an era of global change *Global Change Biology*  
463 **21** 528–49 Online: <http://onlinelibrary.wiley.com/doi/10.1111/gcb.12712/abstract>
- 464 Anderson-Teixeira K J, Wang M M H, McGarvey J C, Herrmann V, Tepley A J, Bond-Lamberty B and  
465 LeBauer D S 2018 ForC: A global database of forest carbon stocks and fluxes *Ecology* **99** 1507–7 Online:  
466 <http://doi.wiley.com/10.1002/ecy.2229>
- 467 Anderson-Teixeira K J, Wang M M H, McGarvey J C and LeBauer D S 2016 Carbon dynamics of mature  
468 and regrowth tropical forests derived from a pantropical database (TropForC-db) *Global Change Biology* **22**  
469 1690–709 Online: <http://onlinelibrary.wiley.com/doi/10.1111/gcb.13226/abstract>
- 470 Baldocchi D, Falge E, Gu L, Olson R, Hollinger D, Running S, Anthoni P, Bernhofer C, Davis K, Evans R,  
471 Fuentes J, Goldstein A, Katul G, Law B, Lee X, Malhi Y, Meyers T, Munger W, Oechel W, Paw K T,  
472 Pilegaard K, Schmid H P, Valentini R, Verma S, Vesala T, Wilson K and Wofsy S 2001 FLUXNET: A New  
473 Tool to Study the Temporal and Spatial Variability of Ecosystem-Scale Carbon Dioxide, Water Vapor, and

- 474 Energy Flux Densities *Bulletin of the American Meteorological Society* **82** 2415–34 Online:  
475 [http://journals.ametsoc.org/doi/abs/10.1175/1520-0477\(2001\)082%3C2415:FANTTS%3E2.3.CO;2](http://journals.ametsoc.org/doi/abs/10.1175/1520-0477(2001)082%3C2415:FANTTS%3E2.3.CO;2)
- 476 Banbury Morgan B, Herrmann V, Kunert N, Bond-Lamberty B, Muller-Landau H C and Anderson-Teixeira  
477 K J Global patterns of forest autotrophic carbon fluxes *Global Change Biology*
- 478 Bond-Lamberty B and Thomson A 2010 A global database of soil respiration data *Biogeosciences* **7** 1915–26  
479 Online: <http://www.biogeosciences.net/7/1915/2010/>
- 480 Chave J, Davies S J, Phillips O L, Lewis S L, Sist P, Schepaschenko D, Armston J, Baker T R, Coomes D,  
481 Disney M, Duncanson L, Héault B, Labrière N, Meyer V, Réjou-Méchain M, Scipal K and Saatchi S 2019  
482 Ground Data are Essential for Biomass Remote Sensing Missions *Surveys in Geophysics* **40** 863–80 Online:  
483 <https://doi.org/10.1007/s10712-019-09528-w>
- 484 Clark D B, Castro C S, Alvarado L D A and Read J M 2004 Quantifying mortality of tropical rain forest  
485 trees using high-spatial-resolution satellite data *Ecology Letters* **7** 52–9 Online:  
486 <https://onlinelibrary.wiley.com/doi/abs/10.1046/j.1461-0248.2003.00547.x>
- 487 Cook-Patton S C, Leavitt S M, Gibbs D, Harris N L, Lister K, Anderson-Teixeira K J, Briggs R D, Chazdon  
488 R L, Crowther T W, Ellis P W, Griscom H P, Herrmann V, Holl K D, Houghton R A, Larrosa C, Lomax G,  
489 Lucas R, Madsen P, Malhi Y, Paquette A, Parker J D, Paul K, Routh D, Roxburgh S, Saatchi S, Hoogen J  
490 van den, Walker W S, Wheeler C E, Wood S A, Xu L and Griscom B W 2020 Mapping carbon accumulation  
491 potential from global natural forest regrowth *Nature* **585** 545–50 Online:  
492 <http://www.nature.com/articles/s41586-020-2686-x>
- 493 Curtis P G, Slay C M, Harris N L, Tyukavina A and Hansen M C 2018 Classifying drivers of global forest  
494 loss *Science* **361** 1108–11 Online: <http://science.sciencemag.org/content/361/6407/1108>
- 495 Goldstein A, Turner W R, Spawn S A, Anderson-Teixeira K J, Cook-Patton S, Fargione J, Gibbs H K,  
496 Griscom B, Hewson J H, Howard J F, Ledezma J C, Page S, Koh L P, Rockström J, Sanderman J and Hole  
497 D G 2020 Protecting irrecoverable carbon in Earth's ecosystems *Nature Climate Change* 1–9 Online:  
498 <http://www.nature.com/articles/s41558-020-0738-8>
- 499 Grassi G, House J, Dentener F, Federici S, Elzen M den and Penman J 2017 The key role of forests in  
500 meeting climate targets requires science for credible mitigation *Nature Climate Change* **7** 220–6 Online:  
501 <https://www.nature.com/articles/nclimate3227>
- 502 Griscom B W, Adams J, Ellis P W, Houghton R A, Lomax G, Miteva D A, Schlesinger W H, Shoch D,  
503 Siikamäki J V, Smith P, Woodbury P, Zganjar C, Blackman A, Campari J, Conant R T, Delgado C, Elias P,  
504 Gopalakrishna T, Hamsik M R, Herrero M, Kiesecker J, Landis E, Laestadius L, Leavitt S M, Minnemeyer S,  
505 Polasky S, Potapov P, Putz F E, Sanderman J, Silvius M, Wollenberg E and Fargione J 2017 Natural climate  
506 solutions *Proceedings of the National Academy of Sciences* **114** 11645–50 Online:  
507 <http://www.pnas.org/lookup/doi/10.1073/pnas.1710465114>
- 508 Hansen M C, Potapov P V, Moore R, Hancher M, Turubanova S A, Tyukavina A, Thau D, Stehman S V,  
509 Goetz S J, Loveland T R, Kommareddy A, Egorov A, Chini L, Justice C O and Townshend J R G 2013  
510 High-Resolution Global Maps of 21st-Century Forest Cover Change *Science* **342** 850–3 Online:  
511 <http://www.sciencemag.org/cgi/doi/10.1126/science.1244693>
- 512 Johnson D J, Needham J, Xu C, Massoud E C, Davies S J, Anderson-Teixeira K J, Bunyavejchewin S,

- 513 Chambers J Q, Chang-Yang C-H, Chiang J-M, Chuyong G B, Condit R, Cordell S, Fletcher C, Giardina C P,  
 514 Giambelluca T W, Gunatilleke N, Gunatilleke S, Hsieh C-F, Hubbell S, Inman-Narahari F, Kassim A R,  
 515 Katabuchi M, Kenfack D, Litton C M, Lum S, Mohamad M, Nasardin M, Ong P S, Ostertag R, Sack L,  
 516 Swenson N G, Sun I F, Tan S, Thomas D W, Thompson J, Umaña M N, Uriarte M, Valencia R, Yap S,  
 517 Zimmerman J, McDowell N G and McMahon S M 2018 Climate sensitive size-dependent survival in tropical  
 518 trees *Nature Ecology & Evolution* **2** 1436–42 Online: <http://www.nature.com/articles/s41559-018-0626-z>
- 519 Krause A, Pugh T A M, Bayer A D, Li W, Leung F, Bondeau A, Doelman J C, Humpenöder F, Anthoni P,  
 520 Bodirsky B L, Ciais P, Müller C, Murray-Tortarolo G, Olin S, Popp A, Sitch S, Stehfest E and Arneth A  
 521 2018 Large uncertainty in carbon uptake potential of land-based climate-change mitigation efforts *Global  
 522 Change Biology* **24** 3025–38 Online: <https://onlinelibrary.wiley.com/doi/abs/10.1111/gcb.14144>
- 523 Leitold V, Morton D C, Longo M, dos-Santos M N, Keller M and Scaranello M 2018 El Niño drought  
 524 increased canopy turnover in Amazon forests *New Phytologist* **219** 959–71 Online:  
 525 <http://doi.wiley.com/10.1111/nph.15110>
- 526 Li X and Xiao J 2019 Mapping Photosynthesis Solely from Solar-Induced Chlorophyll Fluorescence: A  
 527 Global, Fine-Resolution Dataset of Gross Primary Production Derived from OCO-2 *Remote Sensing* **11** 2563  
 528 Online: <https://www.mdpi.com/2072-4292/11/21/2563>
- 529 Lutz J A, Furniss T J, Johnson D J, Davies S J, Allen D, Alonso A, Anderson-Teixeira K J, Andrade A,  
 530 Baltzer J, Becker K M L, Blomdahl E M, Bourg N A, Bunyavejchewin S, Burslem D F R P, Cansler C A,  
 531 Cao K, Cao M, Cárdenas D, Chang L-W, Chao K-J, Chao W-C, Chiang J-M, Chu C, Chuyong G B, Clay K,  
 532 Condit R, Cordell S, Dattaraja H S, Duque A, Ewango C E N, Fischer G A, Fletcher C, Freund J A,  
 533 Giardina C, Germain S J, Gilbert G S, Hao Z, Hart T, Hau B C H, He F, Hector A, Howe R W, Hsieh C-F,  
 534 Hu Y-H, Hubbell S P, Inman-Narahari F M, Itoh A, Janík D, Kassim A R, Kenfack D, Korte L, Král K,  
 535 Larson A J, Li Y, Lin Y, Liu S, Lum S, Ma K, Makana J-R, Malhi Y, McMahon S M, McShea W J,  
 536 Memiaghe H R, Mi X, Morecroft M, Musili P M, Myers J A, Novotny V, Oliveira A de, Ong P, Orwig D A,  
 537 Ostertag R, Parker G G, Patankar R, Phillips R P, Reynolds G, Sack L, Song G-Z M, Su S-H, Sukumar R,  
 538 Sun I-F, Suresh H S, Swanson M E, Tan S, Thomas D W, Thompson J, Uriarte M, Valencia R, Vicentini A,  
 539 Vrška T, Wang X, Weiblen G D, Wolf A, Wu S-H, Xu H, Yamakura T, Yap S and Zimmerman J K 2018  
 540 Global importance of large-diameter trees *Global Ecology and Biogeography* **27** 849–64 Online:  
 541 <https://onlinelibrary.wiley.com/doi/abs/10.1111/geb.12747>
- 542 Luyssaert S, Inglima I, Jung M, Richardson A D, Reichstein M, Papale D, Piao S L, Schulze E-D, Wingate L,  
 543 Matteucci G, Aragao L, Aubinet M, Beer C, Bernhofer C, Black K G, Bonal D, Bonnefond J-M, Chambers J,  
 544 Ciais P, Cook B, Davis K J, Dolman A J, Gielen B, Goulden M, Grace J, Granier A, Grelle A, Griffis T,  
 545 Grünwald T, Guidolotti G, Hanson P J, Harding R, Hollinger D Y, Hutyra L R, Kolari P, Kruijt B, Kutsch  
 546 W, Lagergren F, Laurila T, Law B E, Maire G L, Lindroth A, Loustau D, Malhi Y, Mateus J, Migliavacca M,  
 547 Misson L, Montagnani L, Moncrieff J, Moors E, Munger J W, Nikinmaa E, Ollinger S V, Pita G, Rebmann  
 548 C, Roupsard O, Saigusa N, Sanz M J, Seufert G, Sierra C, Smith M-L, Tang J, Valentini R, Vesala T and  
 549 Janssens I A 2007 CO<sub>2</sub> balance of boreal, temperate, and tropical forests derived from a global database  
 550 *Global Change Biology* **13** 2509–37 Online:  
 551 <http://onlinelibrary.wiley.com/doi/abs/10.1111/j.1365-2486.2007.01439.x>
- 552 McDowell N G, Allen C D, Anderson-Teixeira K, Aukema B H, Bond-Lamberty B, Chini L, Clark J S,  
 553 Dietze M, Grossiord C, Hanbury-Brown A, Hurtt G C, Jackson R B, Johnson D J, Kueppers L, Lichstein J

- 554 W, Ogle K, Poulter B, Pugh T A M, Seidl R, Turner M G, Uriarte M, Walker A P and Xu C 2020 Pervasive  
555 shifts in forest dynamics in a changing world *Science* **368** Online:  
556 <https://science.sciencemag.org/content/368/6494/eaaz9463>
- 557 Pan Y, Birdsey R A, Fang J, Houghton R, Kauppi P E, Kurz W A, Phillips O L, Shvidenko A, Lewis S L,  
558 Canadell J G, Ciais P, Jackson R B, Pacala S, McGuire A D, Piao S, Rautiainen A, Sitch S and Hayes D  
559 2011 A Large and Persistent Carbon Sink in the World's Forests *Science* **333** 988–93 Online:  
560 <http://www.sciencemag.org/content/early/2011/07/27/science.1201609.abstract>
- 561 Pugh T A M, Lindeskog M, Smith B, Poulter B, Arneth A, Haverd V and Calle L 2019 Role of forest  
562 regrowth in global carbon sink dynamics *Proceedings of the National Academy of Sciences* **116** 4382–7  
563 Online: <http://www.pnas.org/lookup/doi/10.1073/pnas.1810512116>
- 564 Requena Suarez D, Rozendaal D M A, Sy V D, Phillips O L, Alvarez-Dávila E, Anderson-Teixeira K,  
565 Araujo-Murakami A, Arroyo L, Baker T R, Bongers F, Brienen R J W, Carter S, Cook-Patton S C,  
566 Feldpausch T R, Griscom B W, Harris N, Héault B, Coronado E N H, Leavitt S M, Lewis S L, Marimon B  
567 S, Mendoza A M, N'dja J K, N'Guessan A E, Poorter L, Qie L, Rutishauser E, Sist P, Sonké B, Sullivan M J  
568 P, Vilanova E, Wang M M H, Martius C and Herold M 2019 Estimating aboveground net biomass change for  
569 tropical and subtropical forests: Refinement of IPCC default rates using forest plot data *Global Change  
570 Biology* **25** 3609–24 Online: <http://onlinelibrary.wiley.com/doi/abs/10.1111/gcb.14767>
- 571 Schepaschenko D, Chave J, Phillips O L, Lewis S L, Davies S J, Réjou-Méchain M, Sist P, Scipal K, Perger  
572 C, Herault B, Labrière N, Hofhansl F, Affum-Baffoe K, Aleinikov A, Alonso A, Amani C, Araujo-Murakami  
573 A, Armston J, Arroyo L, Ascarrunz N, Azevedo C, Baker T, Bałazy R, Bedeau C, Berry N, Bilous A M,  
574 Bilous S Y, Bissiengou P, Blanc L, Bobkova K S, Braslavskaya T, Brienen R, Burslem D F R P, Condit R,  
575 Cuni-Sánchez A, Danilina D, Torres D del C, Derroire G, Descroix L, Sotta E D, d'Oliveira M V N, Dresel C,  
576 Erwin T, Evdokimenko M D, Falck J, Feldpausch T R, Foli E G, Foster R, Fritz S, Garcia-Abril A D,  
577 Gornov A, Gornova M, Gothard-Bassébé E, Gourlet-Fleury S, Guedes M, Hamer K C, Susanty F H, Higuchi  
578 N, Coronado E N H, Hubau W, Hubbell S, Ilstedt U, Ivanov V V, Kanashiro M, Karlsson A, Karminov V N,  
579 Killeen T, Koffi J-C K, Konovalova M, Kraxner F, Krejza J, Krisnawati H, Krivobokov L V, Kuznetsov M A,  
580 Lakyda I, Lakyda P I, Licona J C, Lucas R M, Lukina N, Lussetti D, Malhi Y, Manzanera J A, Marimon B,  
581 Junior B H M, Martinez R V, Martynenko O V, Matsala M, Matyashuk R K, Mazzei L, Memiaghe H,  
582 Mendoza C, Mendoza A M, Morozik O V, Mukhortova L, Musa S, Nazimova D I, Okuda T, Oliveira L C,  
583 et al 2019 The Forest Observation System, building a global reference dataset for remote sensing of forest  
584 biomass *Scientific Data* **6** 1–11 Online: <http://www.nature.com/articles/s41597-019-0196-1>
- 585 Song X-P, Hansen M C, Stehman S V, Potapov P V, Tyukavina A, Vermote E F and Townshend J R 2018  
586 Global land change from 1982 to 2016 *Nature* **560** 639–43 Online:  
587 <http://www.nature.com/articles/s41586-018-0411-9/>
- 588 Taylor P G, Cleveland C C, Wieder W R, Sullivan B W, Doughty C E, Dobrowski S Z and Townsend A R  
589 2017 Temperature and rainfall interact to control carbon cycling in tropical forests ed L Liu *Ecology Letters*  
590 **20** 779–88 Online: <http://doi.wiley.com/10.1111/ele.12765>